*Atmospheric Chemistry Experiment*

# ACE Mission Information for Public Data Release

| | | | |
|---|---|---|---|
| **Prepared by:** | Ryan Hughes<br>*Operations Specialist* | **Document Number:** | ACE-SOC 0025 |
| | | **Revision:** | - |
| **Approved by:** | Peter Bernath<br>*Mission Scientist* | | |
| | | **Issue Date:** | Jun 25, 2012 |

**Atmospheric Chemistry Experiment**
**Science Operations Center**
**Department of Chemistry**
**University of Waterloo**
**Waterloo, ON**
**Canada, N2L 3G1**

www.ace.uwaterloo.ca

# Table of Contents


*1. SUMMARY OF DATA RELEASE AND DOCUMENTATION ..... 5*
*1.1. CSA Acknowledgement ..... 5*
*2. BACKGROUND INFORMATION ABOUT THE ACE MISSION ..... 6*
*2.1. Mission Overview ..... 6*
*2.2. Orbit Information ..... 8*
*2.3. Instrument Summary ..... 8*
*2.4. How Measurements are Taken ..... 10*
*2.4.1. Method ..... 10*
*2.5. Sunrise/Sunset Nomenclature ..... 11*
*2.6. Measurement Coverage ..... 11*
*2.7. Beta Angle (β) ..... 13*
*2.7.1. What is the beta angle? ..... 13*
*2.7.2. Why does the beta angle matter? ..... 14*
*2.7.3. Summary of Measurement Constraints ..... 17*
*3. ACE MEASUREMENTS ..... 19*
*3.1. Baseline Chemical Species ..... 19*
*3.2. Known Data Issues for ACE measurements ..... 21*
*3.3. ACE netCDF File Format Description ..... 22*
*3.4. Public Release (Level 2) Version Details & ReadMe Files ..... 23*
*3.4.1. ACE-FTS Data Version 2.2, Version 2.2 Ozone Update & Version 2.2 $N_2O_5$ Update ReadMe ..... 23*
*3.4.2. ACE-MAESTRO Data Version 1.2 ReadMe ..... 24*
*3.4.3. Historical ACE-FTS ReadMe Files ..... 27*
*3.4.3.1. ACE-FTS Data Version 1.0 ReadMe ..... 27*
*3.4.3.2. ACE-FTS Data Version 2.0 ReadMe ..... 28*
*3.4.3.3. ACE-FTS Data Version 2.1 ReadMe ..... 30*
**REFERENCES ..... 32**
**APPENDIX A: GLOSSARY ..... 36**
**APPENDIX B: ACRONYM LIST ..... 37**
**APPENDIX C: MICROWINDOW LIST ..... 38**

# List of Figures

Figure 1: A typical occultation sequence of atmospheric transmission spectra from the ACE-FTS with the retrieved tangent heights given on the right side ..... 7
Figure 2: The ACE satellite (SCISAT). The baseplate is about 1 m in diameter and the total satellite mass is about 250 kg. Figure courtesy of Bristol Aerospace. ..... 9
Figure 3: A schematic diagram of how an ACE sunset measurement is obtained. For a sunrise the satellite travels in the opposite direction (upward). Figure courtesy of Ray Nassar. ..... 10
Figure 4: Occultation latitudes for ACE throughout one year on orbit. The red and blue lines indicate locations for sunrise and sunset occultations, respectively. The grey line shows the beta angle associated with the measurement. Note that by design, the latitudes of the ACE observations repeat every year, but the longitude of the occultations change from year to year..... 12
Figure 5: A description of how the beta (β) angle is calculated ..... 13
Figure 6: A diagram of SCISAT at a low beta angle (left) and at high beta angle (right). The reader is the looking at this figure from the location of the Sun. (Diagram not drawn to scale). ..... 14
Figure 7: Opportunities for occultation measurements throughout a typical year..... 15
Figure 8: The measurement locations of a low beta occultation (sr10400, 2005-07-18 17:29 UTC, β=-0.76°) in the South-East Pacific. A vertical line is drawn from the measurement location (i.e. tangent height) to the ground. The ground track of this sr10400 is approximately 7.5km in length. The white line connecting the two red dots indicates a 100 km distance. ..... 16
Figure 9: The measurement locations of a high beta occultation (sr17001, 2006-10-09 12:28 UTC, β=55.68°) near the coast of Greenland. A vertical line is drawn from the measurement location (i.e. tangent height) to the ground. The ground track of sr17001 is approximately 840km in length. The white line connecting the two red dots indicates a 100 km distance. ..... 17

# List of Tables

Table 1: Instruments of the ACE satellite and the data version included in this release ..... 5
Table 2: SCISAT orbit details..... 8
Table 3: Baseline species and parameters from ACE, the instruments that measure them and the altitudes over which they are retrieved ..... 21
Table 4: Signal-to-Noise Weighting of Wavenumber Ranges ..... 38
Table 5: Microwindow list for Pressure/Temperature ..... 39
Table 6: Microwindow list for $H_2O$ ..... 41
Table 7: Interfering molecule(s) for $H_2O$..... 42
Table 8: Microwindow list for $O_3$ ..... 43
Table 9: Interfering molecule(s) for $O_3$ ..... 43
Table 10: Microwindow list for $N_2O$ ..... 44
Table 11: Interfering molecule(s) for $N_2O$..... 45
Table 12: Microwindow list for CO..... 45
Table 13: Interfering molecule(s) for CO ..... 46
Table 14: Microwindow list for $CH_4$ ..... 46
Table 15: Microwindow list for NO ..... 48

Table 16: Interfering molecule(s) for NO ..... 48
Table 17: Microwindow list for $NO_2$ ..... 49
Table 18: Microwindow list for $HNO_3$ ..... 49
Table 19: Interfering molecule(s) for $HNO_3$ ..... 50
Table 20: Microwindow list for HF ..... 50
Table 21: Interfering molecule(s) for HF ..... 50
Table 22: Microwindow list for HCl ..... 51
Table 23: Interfering molecule(s) for HCl ..... 51
Table 24: Microwindow list for OCS ..... 51
Table 25: Interfering molecule(s) for OCS ..... 52
Table 26: Microwindow list for $N_2O_5$ ..... 52
Table 27: Interfering molecule(s) for $N_2O_5$ ..... 52
Table 28: Microwindow list for $ClONO_2$ ..... 52
Table 29: Interfering molecule(s) for $ClONO_2$ ..... 52
Table 30: Microwindow list for HCN ..... 53
Table 31: Microwindow list for $CH_3Cl$ ..... 53
Table 32: Interfering molecule(s) for $CH_3Cl$ ..... 53
Table 33: Microwindow list for $CF_4$ ..... 53
Table 34: Interfering molecule(s) for $CF_4$ ..... 53
Table 35: Microwindow list for $CCl_2F_2$ (CFC-12) ..... 54
Table 36: Interfering molecule(s) for $CCl_2F_2$ (CFC-12) ..... 54
Table 37: Microwindow list for $CCl_3F$ (CFC-11) ..... 54
Table 38: Interfering molecule(s) for $CCl_3F$ (CFC-11) ..... 54
Table 39: Microwindow list for $COF_2$ ..... 54
Table 40: Interfering molecule(s) for $COF_2$ ..... 54
Table 41: Microwindow list for $C_2H_6$ ..... 55
Table 42: Interfering molecule(s) for $C_2H_6$ ..... 55
Table 43: Microwindow list for $C_2H_2$ ..... 55
Table 44: Interfering molecule(s) for $C_2H_2$ ..... 55
Table 45: Microwindow list for $CHF_2Cl$ ..... 55
Table 46: Interfering molecule(s) for $CHF_2Cl$ ..... 55
Table 47: Microwindow list for $SF_6$ ..... 55
Table 48: Interfering molecule(s) for $SF_6$ ..... 56
Table 49: Microwindow list for ClO ..... 56
Table 50: Interfering molecule(s) for ClO ..... 56
Table 51: Microwindow list for $HO_2NO_2$ ..... 56
Table 52: Microwindow list for $H_2O_2$ ..... 56
Table 53: Microwindow list for HOCl ..... 56
Table 54: Microwindow list for $N_2$ ..... 57
Table 55: Interfering molecule(s) for $N_2$ ..... 57

# 1. Summary of Data Release and Documentation

This document is designed to give data users important background and supporting material to best utilize the data set from the Atmospheric Chemistry Experiment (ACE) satellite mission. This public release is comprised of the altitude profiles of temperature, atmospheric extinction and 14 atmospheric trace gas species ($O_3$, $H_2O$, $N_2O$, $CH_4$, NO, $NO_2$, $HNO_3$, $N_2O_5$, $ClONO_2$, HCl, HF, CO, CFC-11 and CFC-12) provided by the three ACE instruments. These profiles form the baseline Level 2 data set from ACE. Lower level data products, such as Level 1 calibrated spectra or Level 0 raw data recorded by the instruments, are not part of this data release. The specific version numbers for these data are listed below.

| ACE Instrument | Data Version in this Release |
|---|---|
| ACE-FTS | 2.2 + updates for $O_3$ and $N_2O_5$ |
| ACE-MAESTRO | 1.2 |
| ACE-Imagers | 2.2 |

**Table 1: Instruments of the ACE satellite and the data version included in this release**

This document is laid out as follows. Section 2 of this document provides a summary of the ACE instruments, measurements, satellite orbit and measurement technique. In Section 3, detailed information is provided on the data products including file format documentation, "readme files" for each of the data products, lists of known data issues, references to validation studies. An appendix provides the microwindow lists used for the ACE-FTS retrievals.

Prior to working with the ACE data, users are strongly encouraged to read this documentation (including the data product readme files) and the papers describing the retrieval processes for these data products (ACE-FTS: Boone et al. (2005); ACE-MAESTRO: McElroy et al. (2007); and ACE-Imagers; Gilbert et al. (2007) and the data product validation publications (http://www.atmos-chem-phys.net/special_issue114.html).

## 1.1. CSA Acknowledgement

In any publications using ACE data, it is important to acknowledge the Canadian Space Agency for the funding of the SCISAT satellite. Any text that recognizes the Canadian Space Agency as funding the ACE Mission is permitted, but we have provided a sample to use that meets this requirement. This simple statement has been used in many publications with ACE data:

*The Atmospheric Chemistry Experiment (ACE), also known as SCISAT, is a Canadian-led mission mainly supported by the Canadian Space Agency.*

# 2. Background Information about the ACE Mission

## 2.1. Mission Overview

*The text in this section is adapted from: Bernath, P. (2001), The Atmospheric Chemistry Experiment (ACE): An Overview, Spectroscopy from Space, Kluwer Academic Publishers, pp. 147-161.*

The Atmospheric Chemistry Experiment (ACE) is a Canadian satellite mission for remote sensing of the Earth's atmosphere that was launched into a high-inclination (74°), circular low-earth (650 km from the surface) orbit on August 12, 2003 (Bernath et al., 2006). This orbit gives SCISAT coverage of tropical, mid-latitude, and polar regions, ranging from latitudes 85°N to 85°S, allowing it to study a range of atmospheric processes. The main goal of ACE is to study the atmospheric chemistry and dynamics that affect stratospheric ozone depletion in the Arctic, but ACE measurements are also being used to study ozone depletion in the Antarctic, the relationship between chemistry and climate change, the atmospheric effects of biomass burning, the effects of aerosols and clouds on the global energy balance, and many other areas of atmospheric science.

The primary instrument on SCISAT is a high spectral resolution (0.02 $cm^{-1}$, corresponding to ± 25 cm maximum optical path difference) infrared Fourier transform spectrometer (ACE-FTS), operating over a broad wavenumber range (750-4400 $cm^{-1}$). As SCISAT orbits the Earth, the ACE-FTS measures sequences of atmospheric absorption spectra during sunrise and sunset. These spectra, measured in the limb viewing geometry with different slant paths and tangent heights are inverted to obtain vertical profiles of temperature, pressure and volume mixing ratios (VMRs) for dozens of trace gases with a vertical resolution of 3-4 km from the cloud tops (or 5 km in the absence of clouds) up to about 120 km. An example sequence of ACE-FTS spectra is shown in Figure 1.

SCISAT also features a UV-visible-NIR spectrophotometer known as Measurement of Aerosol Extinction in the Stratosphere and Troposphere Retrieved by Occultation (ACE-MAESTRO). ACE-MAESTRO is a dual optical spectrophotometer that was designed to cover the 285-1030 nm spectral region (MAESTRO now covers 400-1030 nm). It has a vertical resolution of 1-2 km and measures primarily ozone, nitrogen dioxide, and aerosol/cloud extinction using solar occultation (McElroy et al., 2007).

In addition, a pair of filtered imagers on board SCISAT (ACE-Imagers) make high signal-to-noise ratio (SNR) measurements at 0.525 and 1.02 μm (Gilbert et al., 2007). Atmospheric extinction profiles derived from the imager sunrise and sunset measurements are used for the monitoring of aerosols and clouds and provide an important diagnostic for the variation of the flux over the solar disk (distorted at low altitudes by atmospheric refraction and the presence of clouds).

The ACE-FTS mission concept is based on the ATMOS (Atmospheric Trace MOlecule Spectroscopy) instrument that NASA flew four times (1985, 1992, 1993, and 1994) on the Space Shuttle but the ACE-FTS has been miniaturized by nearly a factor of 10 in mass, power, and volume as compared to ATMOS. With fewer than 400 occultations, ATMOS has made and continues to make valuable contributions to atmospheric science. The ACE

instruments, ACE-FTS, ACE-MAESTRO and ACE-Imagers, have measured 25,500 occultations up to September 2010 and measure about 4,500 occultations per year. In combination, these instruments are now providing a wealth of scientific data that will be used to help improve our understanding of processes in the Earth's atmosphere for years to come.

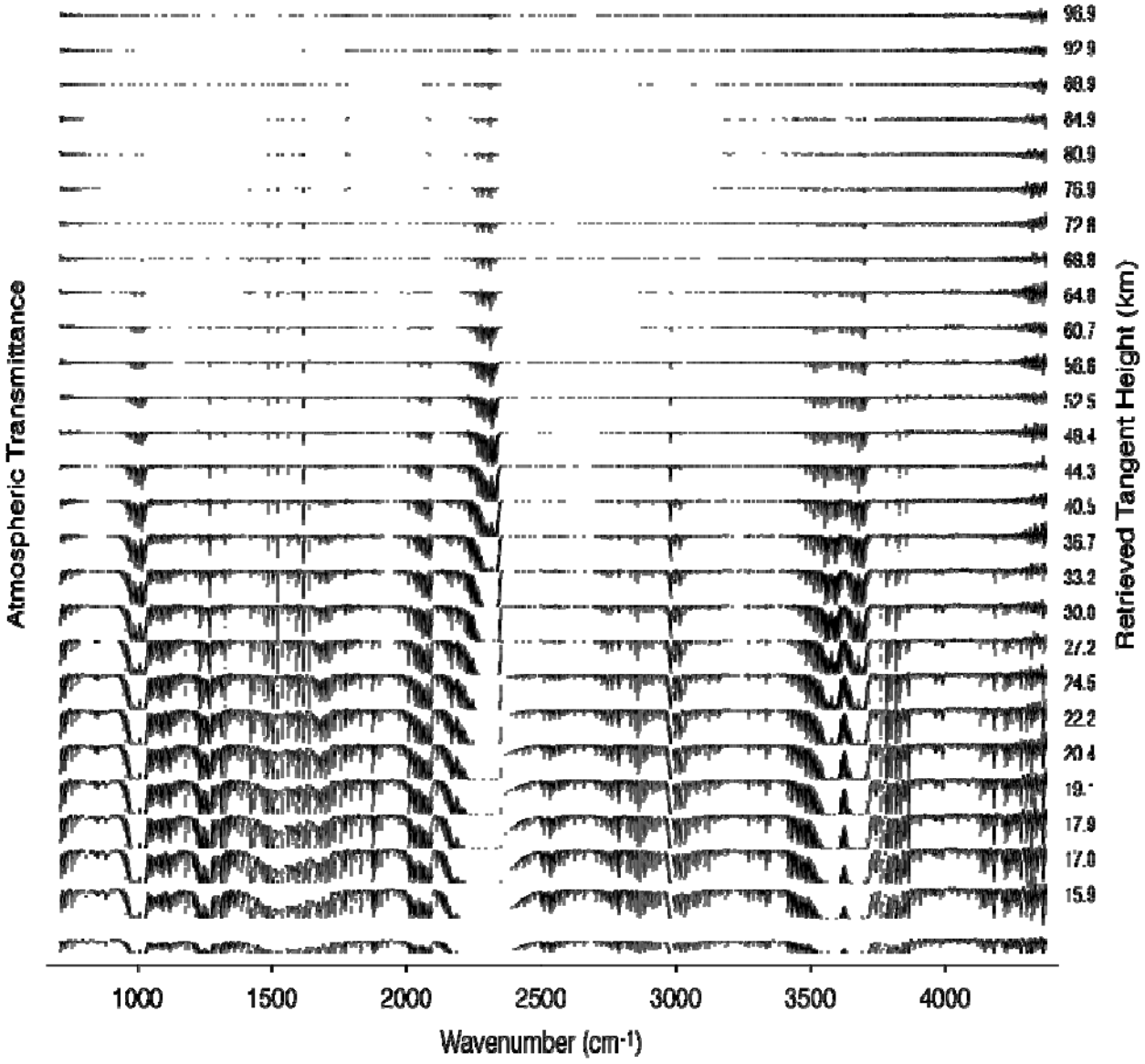


**Figure 1: A typical occultation sequence of atmospheric transmission spectra from the ACE-FTS with the retrieved tangent heights given on the right side**

## 2.2. Orbit Information

| | |
|---|---|
| *Inclination* | 74° |
| *Altitude* | 650 km |
| *Orbit Eccentricity* | 0° (circular) |
| *Orbital Period* | 97.7 minutes |
| *Orbital Lifetime* | > 5 Years |

**Table 2: SCISAT orbit details**

## 2.3. Instrument Summary

*This section is adapted from: Bernath, P. (2006), Atmospheric Chemistry Experiment (ACE): Analytical Chemistry from Orbit, Trends in Analytical Chemistry, Vol. 25, No. 7, pp. 647-654.*

A schematic of the SCISAT satellite is shown in Figure 2. The main instrument on SCISAT, ACE-FTS, is a Michelson interferometer of a custom design (Bernath 2006). The interferometer uses two cube corners rotating on a central flex pivot to produce the optical path difference. An "end" mirror inside the interferometer is used to double pass the radiation and increase the optical path difference. The ACE-FTS design is fully compensated for tilt and shear of both moving and stationary optics inside the interferometer. A pointing mirror, controlled by a suntracker servo-loop, locks on the Sun center and tracks it while the instrument is taking measurements. The ACE-FTS has a circular field of view (FOV) of 1.25 mrad, a mass of about 41 kg, and an average power consumption of 37 W. Double-sided interferograms are Fourier transformed on the ground to obtain the desired atmospheric spectra. The ACE-FTS uses two photovoltaic detectors (InSb and HgCdTe), aligned with a dichroic element to have the same field of view. The detectors are cooled to 80-100 K by a passive radiator pointing toward deep space. The SNR of a typical ACE-FTS spectrum is greater than 300 over most of the spectral band.

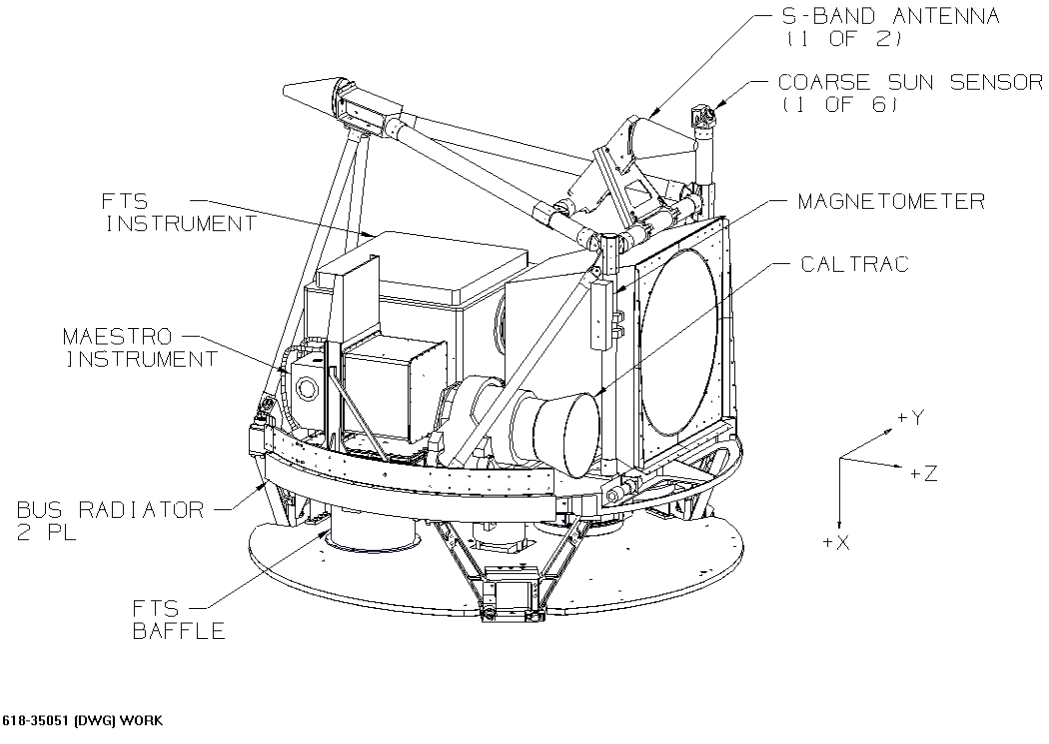


**Figure 2: The ACE satellite (SCISAT). The baseplate is about 1 m in diameter and the total satellite mass is about 250 kg. Figure courtesy of Bristol Aerospace.**

The visible/near infrared imager, ACE-Imagers, has two filter channels at 0.525 and 1.02 μm, chosen to match two of the wavelengths monitored by the SAGE II satellite instrument (Gilbert et al., 2007). The ACE-Imagers also provide an important diagnostic for pointing and for detecting the presence of clouds in the FOV. The detectors in the ACE-Imagers are (effectively) 128 x 128 active pixel sensors made by Fill Factory of Mechelen, Belgium. The total FOV of the ACE-Imagers is 30 mrad, to be compared to the 9 mrad angular diameter of the Sun. The SNR of each solar image is greater than 1000, but the main image suffers from overlap by weak secondary images from optical filters that were not tipped far enough off the optical axis.

ACE-MAESTRO is a small (about 8 kg) spectrophotometer designed to cover the 285–1030 nm region in two overlapping segments (McElroy et al., 2007). The use of two spectrographs (280–550 nm, 500–1030 nm) reduces the stray light and permits simultaneous measurements of the two bands with spectral resolution of 1–2 nm, depending on wavelength. The detectors are 1024 linear EG & G Reticon photodiode arrays. The design is based on a simple concave grating with no moving parts. The entrance slit is held horizontal with respect to the horizon during sunrise. The ACE-FTS, ACE-Imagers and ACE-MAESTRO all share a single Sun-tracker and have approximately the same direction of view. The ACE-MAESTRO SNR is in excess of 1000. While the ACE mission works primarily by solar occultation, ACE-MAESTRO is also able to make near-nadir solar backscatter measurements, like the GOME instrument on the European ERS-2 satellite (Burrows et al., 1999).

The analysis procedures for the ACE instruments use the inherent "self-calibrating" advantage of the solar occultation technique. For each occultation, measurements are collected during the time when rays from the Sun pass well above the Earth's atmosphere (tangent altitudes of 160-225 km). Individual atmospheric measurements (by definition, solar-view measurements with tangent altitudes below 150 km) are divided by an average of the exoatmospheric spectra for the same occultation, thereby removing both the instrumental response and the solar spectral features. For the ACE-FTS, additional measurements are taken during a brief period when the input mirror is deliberately moved off the sun to point to deep space. The deep space measurements are averaged and then subtracted from all "solar-view" measurements for that occultation, in order to correct for self-emission of the instrument. The ACE-FTS spectra are recorded every 2 s during sunrise or sunset. When the Sun is below the horizon, the ACE-MAESTRO records spectra to allow the calculation of the detector dark current. Approximately 60 atmospheric spectra are measured by ACE-MAESTRO during each occultation. Retrieval details for ACE-FTS, ACE-MAESTRO and ACE-Imagers are provided in Boone et al. (2005), McElroy et al. (2007) and Gilbert et al. (2007), respectively.

## 2.4. How Measurements are Taken

### 2.4.1. Method

Solar occultation is a technique in which the transmission of sunlight through the Earth's atmosphere is measured and ratioed to exoatmospheric measurements (solar measurements recorded with no atmospheric attenuation). This is carried out at a series of tangent heights, increasing in altitude during a sunrise or decreasing in altitude during a sunset, as depicted in Figure 3. From each of the atmospheric measurements a slant column is calculated which can contain contributions from multiple atmospheric layers. The slant columns contain sufficient information that when combined and inverted, one can obtain a profile of the atmosphere.

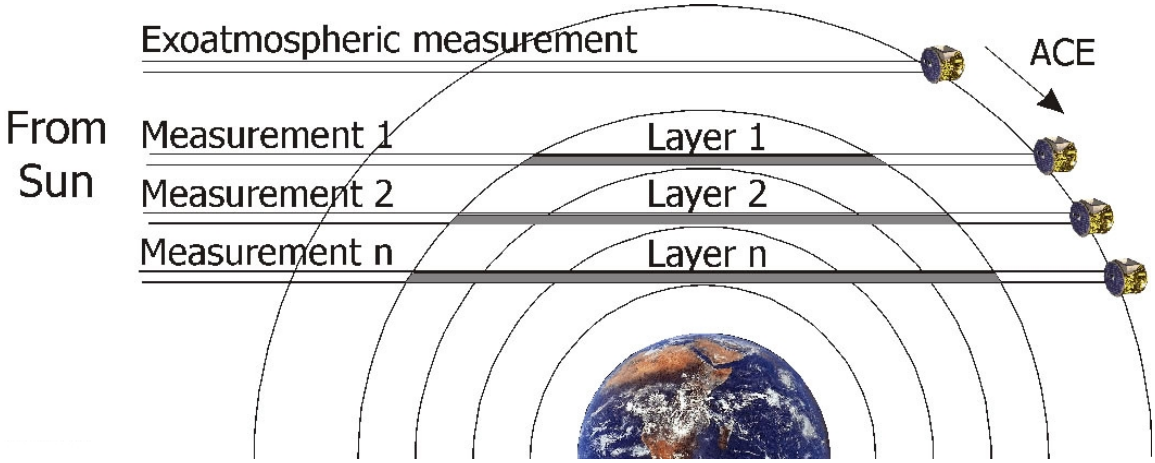


**Figure 3: A schematic diagram of how an ACE sunset measurement is obtained. For a sunrise the satellite travels in the opposite direction (upward). Figure courtesy of Ray Nassar.**

A single occultation consists of pointing the suntracker mirror at the centre of the Sun and taking measurements in the region between high altitudes (i.e., the set of exoatmospheric

measurements used to calibrate the atmospheric measurements) and the Earth's surface (or as close to the surface as possible). The sun tracker mirror stops tracking when the solar intensity level falls below a threshold value, and this effectively limits the ACE occultations to an altitude of 5 km for a cloud-free scene. Occultations vary in length due to the orbit (See Section 2.7) so the number of measurements per occultation and measurement altitudes are not constant. The vertical spacing of the measurements is smallest at low altitudes due to refraction of the Sun's light through the Earth's atmosphere.

## 2.5. Sunrise/Sunset Nomenclature

The sunrise/sunset naming convention is based on the rising and setting of the Sun as viewed from the satellite. The difference between a sunrise and a sunset occultation is the order in which the measurements are taken. For a sunset, the instruments start by taking exoatmospheric measurements then continue taking measurements through the atmosphere until the Sun is no longer visible due to the Earth. For a sunrise, the instruments start by taking measurements of the lower atmosphere and continue taking measurements through the atmosphere until the exoatmospheric measurements are completed. Because a sunset is defined as the setting of the Sun as viewed from the satellite, measurement times don't necessarily correspond to sunsets viewed from the Earth's surface. Likewise, a sunrise as viewed from the satellite may not correspond to a sunrise as viewed from Earth.

## 2.6. Measurement Coverage

The latitude of the ACE occultation measurements is not constant. It changes throughout the year (as shown in Figure 4). It should also be pointed out that there are two periods during the year where there are no measurements for a duration of almost 3 weeks: June and December. During these periods the orbital beta angle is so high that the Sun, as viewed from the satellite, never sets. Beta is the angle between the orbit plane of the satellite and the Earth-Sun vector. The greater the absolute value of this angle, the longer the measurement. See the following Section 2.7 for an explanation of the satellite's beta angle.

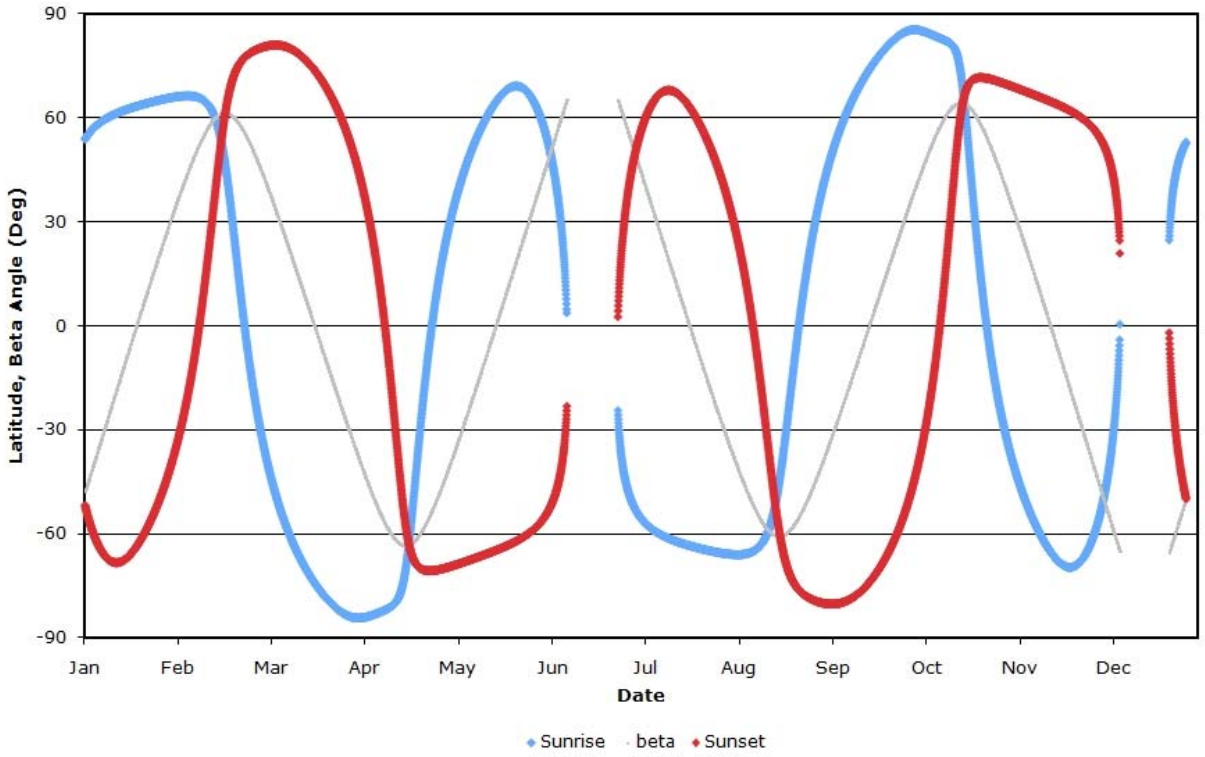


**Figure 4: Occultation latitudes for ACE throughout one year on orbit. The red and blue lines indicate locations for sunrise and sunset occultations, respectively. The grey line shows the beta angle associated with the measurement. Note that by design, the latitudes of the ACE observations repeat every year, but the longitude of the occultations change from year to year.**

## 2.7. Beta Angle (β)

### 2.7.1. What is the beta angle?

The beta angle is the angle between the orbit plane of the satellite and the Earth-Sun vector. Figure 5 shows a diagram of how the beta angle is calculated. The beta angle is a characteristic of the satellite's orbit and changes continuously, but is periodic. The absolute value of the beta angle ranges from 0 to 82.5 degrees (i.e., $0 \leq |\beta| \leq 82.5$) and only reaches its highest value twice per year-during the high beta gaps in June and December. Figure 6 shows the SCISAT orbit at a low beta angle (left), and at a high beta angle (right) as seen from the Sun.

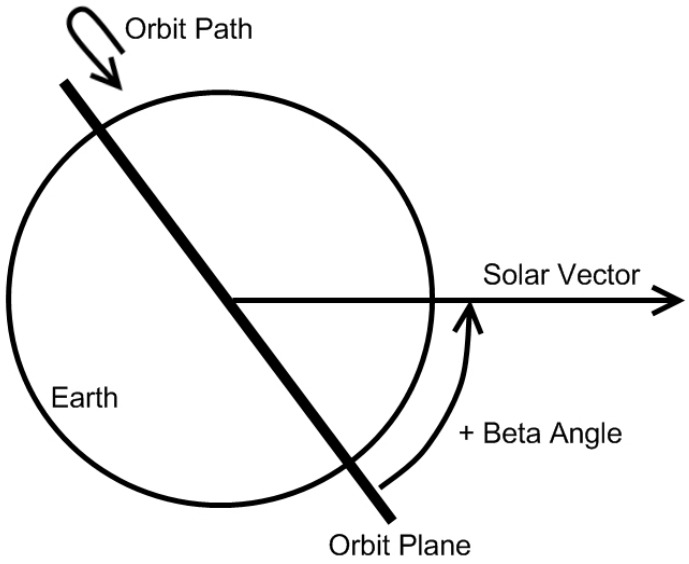


**Figure 5: A description of how the beta (β) angle is calculated**

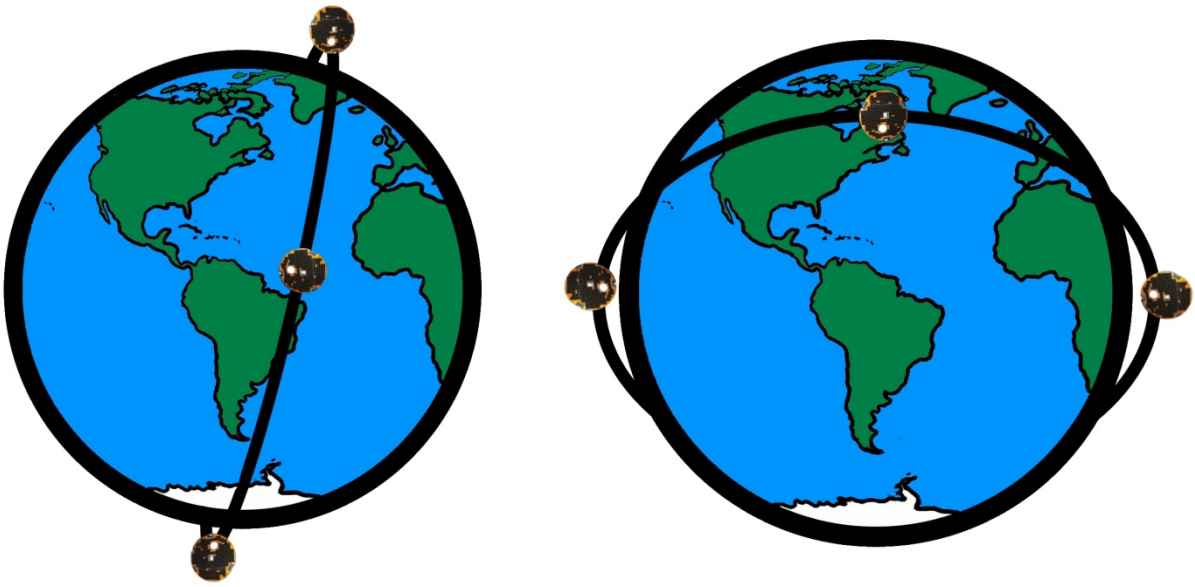

**Figure 6: A diagram of SCISAT at a low beta angle (left) and at high beta angle (right). The reader is the looking at this figure from the location of the Sun. (Diagram not drawn to scale).**

### 2.7.2. Why does the beta angle matter?

The ACE instruments collect a series of measurements over the course of an occultation, each measurement at a different altitude. Analysis of the ACE data exploits the altitude sampling inherent in the solar occultation measurement technique to derive profiles for the atmospheric quantities of interest. The distance between each measurement changes as the beta angle changes. For example, the vertical spacing between ACE-FTS measurements at zero beta angle is approximately 6 km, whereas the vertical spacing at a beta angle of 55° is approximately 2 km. This happens because a beta angle of 0° corresponds to a vertical trajectory for the sunset relative to the horizon, when viewed from the spacecraft. All other beta angles mean that the Sun sets at an oblique angle to the horizon; the Sun therefore takes longer to set and the vertical sampling is smaller for a fixed 2-second sampling time.

The increased rate of vertical sampling for higher beta angles is a benefit for the retrievals, providing better altitude discrimination for the derived profiles. However, the higher data volumes and increased duration of occultation (sunrise and sunset) events also have disadvantages. Figure 7 is a similar plot to Figure 4 but indicates periods in the satellite's orbit where only a subset of the available measurements are actually collected. At low beta angles, occultation durations are short and the associated data volumes are therefore small. As beta angle increases, data volumes increase, and the amounts of onboard storage and available downlink capacity become limiting factors. Also, there are periods where there is not sufficient time during the eclipse part of the orbit to perform the pre-measurement and post-measurement activities. Therefore, at high beta measurement opportunities are routinely skipped in order to avoid exceeding the onboard storage capacity and overlapping command sequences. As shown in Figure 7, at very high beta angles (> 57°) it is common practise to skip more than half of the available measurement opportunities.

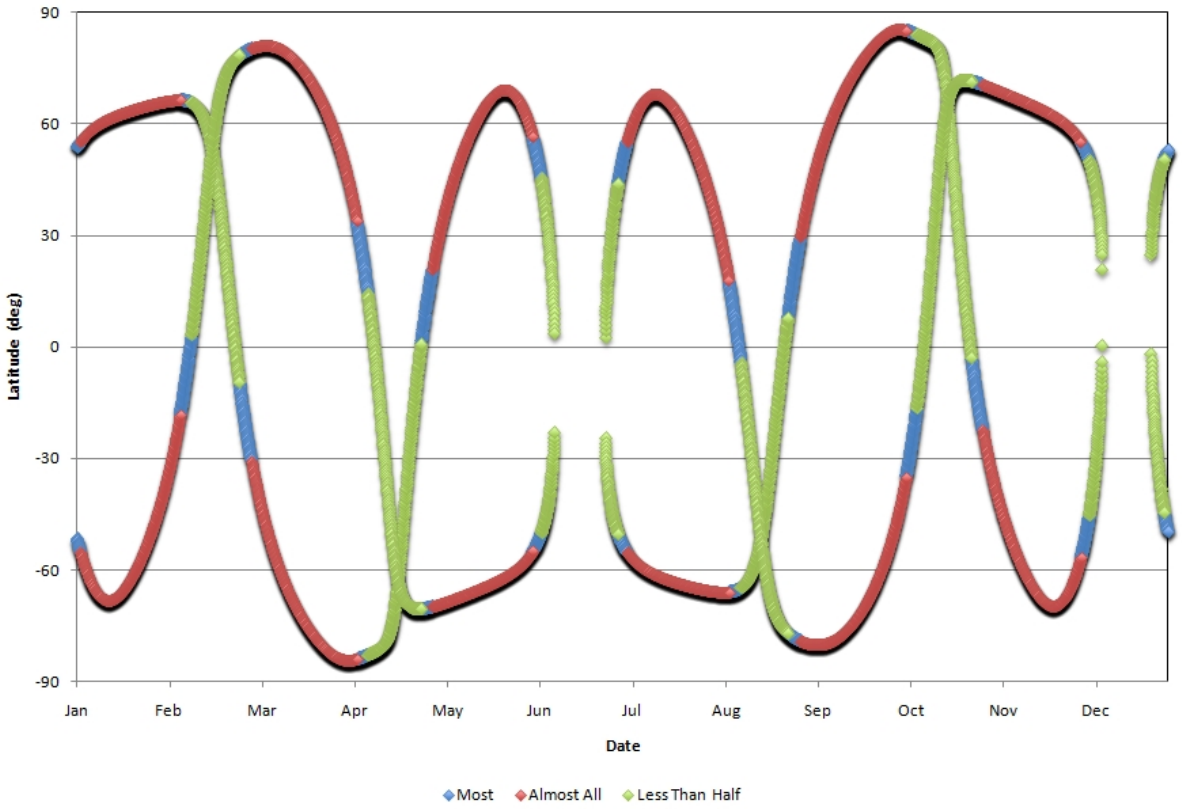


**Figure 7: Opportunities for occultation measurements throughout a typical year**

Another disadvantage of high beta angle measurements arises from the increased occultation duration. Because the satellite moves in its orbit as it performs measurements, the tangent points for the different measurements are "smeared" geographically. Figure 8 shows the degree of smearing for a low beta angle occultation. The degree of smearing for high beta angle occultations can be as high as several hundred kilometers, as shown in Figure 9. When looking at geographical variations of quantities measured by ACE, this smearing could complicate the interpretation and should be kept in mind. Information on the ground locations (latitude and longitude) for each measurement in an occultation is included in the ACE data files.

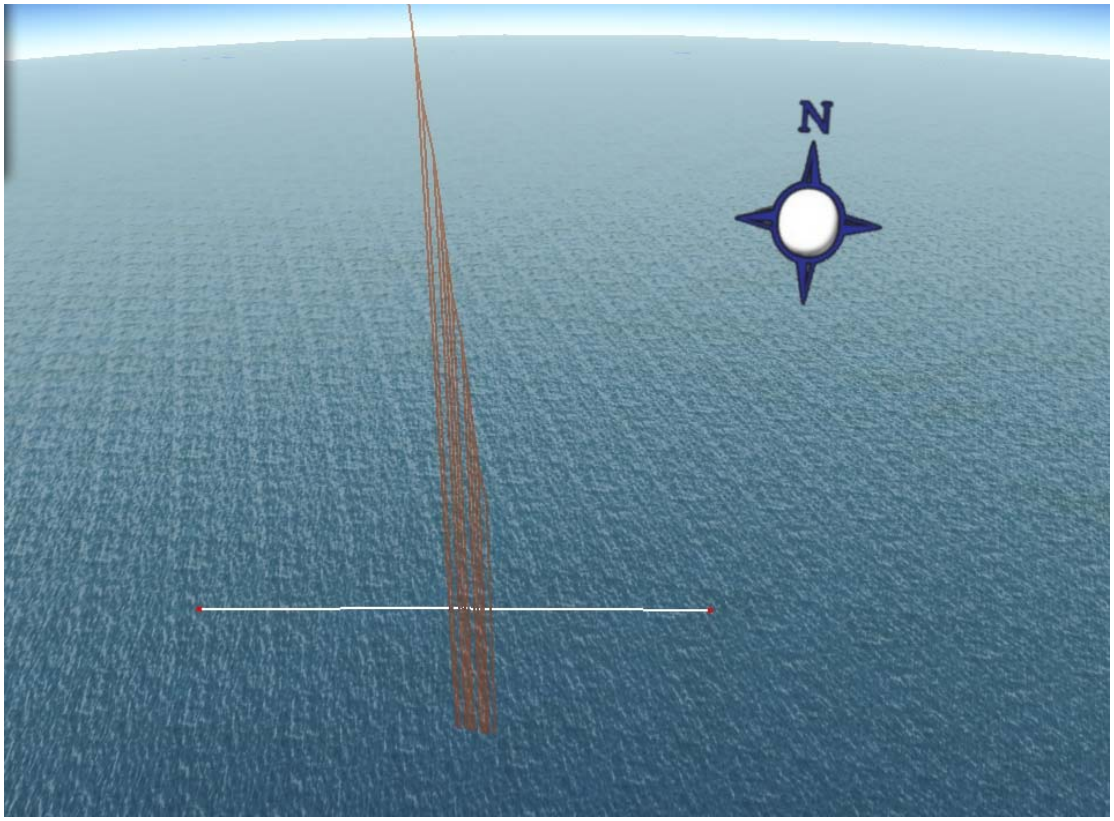


**Figure 8: The measurement locations of a low beta occultation (sr10400, 2005-07-18 17:29 UTC, β=-0.76°) in the South-East Pacific. A vertical line is drawn from the measurement location (i.e. tangent height) to the ground. The ground track of sr10400 is approximately 7.5km in length. The white line connecting the two red dots indicates a 100 km distance.**

Also, as Figure 4 shows, there are two periods during the year (in June and December) when measurements cannot be taken (the gaps in the red and blue curves). During these times, the beta angle is so large that the satellite remains continually in sunlight, and so the satellite does not experience a sunrise or a sunset. Each of these periods is approximately 3 weeks in length.

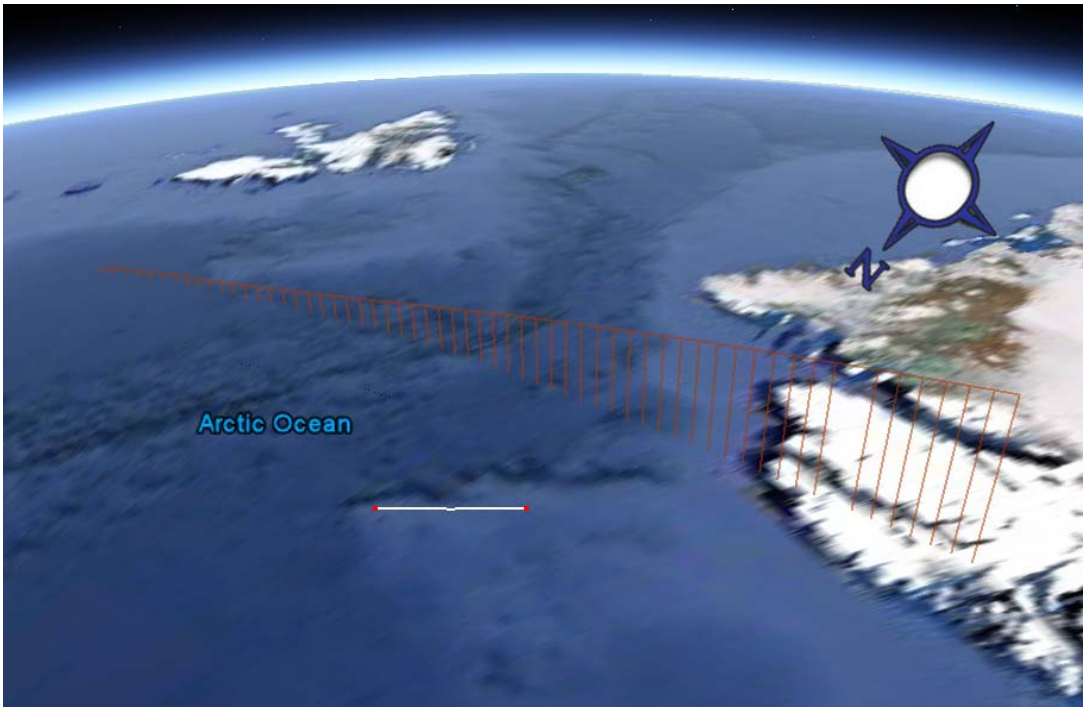


**Figure 9: The measurement locations of a high beta occultation (sr17001, 2006-10-09 12:28 UTC, β=55.68°) near the coast of Greenland. A vertical line is drawn from the measurement location (i.e. tangent height) to the ground. The ground track of sr17001 is approximately 840km in length. The white line connecting the two red dots indicates a 100 km distance.**

### 2.7.3. Summary of Measurement Constraints

Not every measurement opportunity for the ACE instruments is taken. Although an effort is made to take as many measurements as possible, there are times when it is not possible. Below are a few reasons why the satellite may not have data: The reader is referred to Figure 7 for information that complements this discussion.

*High Beta Gap*: This occurs in June and December and lasts approximately 3 weeks each time. No measurements are taken during this time because the spacecraft is in constant sunlight. This occurs when the beta angle is greater than 65° (i.e., $|\beta| > 65°$).

*Single Measurements per Orbit*: At certain beta angles, the spacecraft is only able to take one measurement per orbit. This is because there is not enough time during the eclipse period during the orbit between the measurements to perform the pre-measurement and post-measurement activities. This only happens at beta angles greater than 57° (i.e., $|\beta| > 57°$).

*Downlink Capacity/Spacecraft Storage*: There is only a limited amount of data storage on-board (1.5 GB) the satellite and there are only a few ground stations where data can be retrieved. All of these ground stations are jointly used by ACE and other remote sensing projects. If the data storage gets full, then no more measurements can be taken until some of the data are down-linked to the ground. Also, the spacecraft

may be oriented in such a way that it is not able to obtain a line-of-sight connection with the ground station during an overpass. If this happens, then the spacecraft cannot unload the data to the ground.

*Incomplete Data Transfer from Satellite to the Ground*: sometimes data gets lost or corrupted when it is being transferred to the ground station.

The first three are known before the measurements are scheduled so measurements are scheduled within these constraints but nothing can be done to recover the data when there is an incomplete data transfer.

# 3. ACE Measurements

## 3.1. Baseline Chemical Species

| Molecule | Altitude (km) | Validation Paper Reference | Instrument(s) |
|---|---|---|---|
| $O_3$ | 5 – 95 | Dupuy, E., et al. (2009), **Validation of ozone measurements from the Atmospheric Chemistry Experiment (ACE)**, Atmos. Chem. Phys., 9, 287-343, 2009 | ACE-FTS ACE-MAESTRO |
| $H_2O$ | 5 – 89 | Carleer, M., et al. (2008), **Validation of water vapour profiles from the Atmospheric Chemistry Experiment (ACE)**, Atmos. Chem. Phys. Discuss., 8, 4499-4559, 2008 | ACE-FTS |
| $CH_4$ | 5 – 62 | De Mazière, M., et al. (2008), **Validation of ACE-FTS v2.2 methane profiles from the upper troposphere to lower mesosphere**, Atmos. Chem. Phys., 8, 2421-2435, 2008 | ACE-FTS |
| $N_2O$ | 5 – 60 | Strong, K., et al. (2008),**Validation of ACE-FTS $N_2O$ measurements**, Atmos. Chem. Phys., 8, 4759-4786, 2008 | ACE-FTS |
| $NO_2$ | 13 – 45 | Kerzenmacher, T., et al. (2008), **Validation of $NO_2$ and NO from the Atmospheric Chemistry Experiment (ACE)**, Atmos. Chem. Phys., 8, 5801-5841, 2008 | ACE-FTS ACE-MAESTRO |
| NO | 12 – 105 | Kerzenmacher, T., et al. (2008), **Validation of $NO_2$ and NO from the Atmospheric Chemistry Experiment (ACE)**, Atmos. Chem. Phys., 8, 5801-5841, 2008 | ACE-FTS |
| $HNO_3$ | 5 – 37 | Wolff, M.A., et al. (2008), **Validation of $HNO_3$, $ClONO_2$, and $N_2O_5$ from the Atmospheric Chemistry Experiment Fourier Transform Spectrometer (ACE-FTS)**, Atmos. Chem. Phys., 8, 3529-3562, 2008 | ACE-FTS |

| Molecule | Altitude (km) | Validation Paper Reference | Instrument(s) |
|---|---|---|---|
| HCl | 8 – 57 | Mahieu, E., et al. (2008), **Validation of ACE-FTS v2.2 Measurements of HCl, HF, $CCl_3F$, and $CCl_2F_2$ using space-, balloon- and ground-based instrument observations**, Atmos. Chem. Phys., 8, 6199-6221, 2008 | ACE-FTS |
| HF | 10 – 50 | Mahieu, E., et al. (2008), **Validation of ACE-FTS v2.2 Measurements of HCl, HF, $CCl_3F$, and $CCl_2F_2$ using space-, balloon- and ground-based instrument observations**, Atmos. Chem. Phys., 8, 6199-6221, 2008 | ACE-FTS |
| CO | 5 – 105 | Clerbaux, C., et al. (2008), **CO measurements from the ACE-FTS satellite instrument: data analysis and validation using ground-based, airborne and spaceborne observations**, Atmos. Chem. Phys., 8, 2569-2594, 2008 | ACE-FTS |
| CFC-11 ($CCl_3F$) | 5 – 22 | Mahieu, E., et al. (2008), **Validation of ACE-FTS v2.2 Measurements of HCl, HF, $CCl_3F$, and $CCl_2F_2$ using space-, balloon- and ground-based instrument observations**, Atmos. Chem. Phys., 8, 6199-6221, 2008 | ACE-FTS |
| CFC-12 ($CCl_2F_2$) | 6 – 28 | Mahieu, E., et al. (2008), **Validation of ACE-FTS v2.2 Measurements of HCl, HF, $CCl_3F$, and $CCl_2F_2$ using space-, balloon- and ground-based instrument observations**, Atmos. Chem. Phys., 8, 6199-6221, 2008 | ACE-FTS |
| $N_2O_5$ | 15 – 40 | Wolff, M.A., et al. (2008), **Validation of $HNO_3$, $ClONO_2$, and $N_2O_5$ from the Atmospheric Chemistry Experiment Fourier Transform Spectrometer (ACE-FTS)**, Atmos. Chem. Phys., 8, 3529-3562, 2008 | ACE-FTS |

| Molecule | Altitude (km) | Validation Paper Reference | Instrument(s) |
|---|---|---|---|
| $ClONO_2$ | 12 – 35 | Wolff, M.A., et al. (2008), **Validation of $HNO_3$, $ClONO_2$, and $N_2O_5$ from the Atmospheric Chemistry Experiment Fourier Transform Spectrometer (ACE-FTS)**, Atmos. Chem. Phys., 8, 3529-3562, 2008 | ACE-FTS |
| Temperature | 0 – 150 | Sica, R.J., et al. (2008),**Validation of the Atmospheric Chemistry Experiment (ACE) version 2.2 temperature using ground based and space-borne measurements**, Atmos. Chem. Phys., 8, 35-62, 2008 | ACE-FTS |
| Atmospheric Extinction | 0 – 150 | Vanhellemont, F., et al. (2008),**Validation of 525 nm and 1020 nm aerosol extinction profiles derived from ACE Imager data: comparisons with GOMOS, SAGE II, SAGE III, POAM III, and OSIRIS**, Atmos. Chem. Phys., 8, 2027-2037, 2008 | ACE-Imagers |

**Table 3: Baseline species and parameters from ACE, the instruments that measure them and the altitudes over which they are retrieved**

## 3.2. Known Data Issues for ACE measurements

*The ACE Science Operations phase started on February 21, 2004*. ACE measurements taken in late 2003 and early 2004 were done as part of the Satellite Commissioning phase. Occultations measured prior to January 10, 2004 were for calibration and these occultations should not be used at all. Measurements taken during the Science Commissioning period, during January and most of February 2004, generally should not be used. Since February 21, 2004, there have been a few instances where there were issues with the data and the occultations from these periods should be avoided or used with caution. For example, detector temperatures which are higher than nominal degrade the SNR performance of the ACE-FTS and this can negatively impact the retrievals.

A list of data issues for all ACE instruments is maintained by the ACE team and can be accessed at:
**https://databace.uwaterloo.ca/validation/data_issues.php**

To report data issues, please use the web form located at:
**https://databace.uwaterloo.ca/validation/data_issues_report_form.php.**

## 3.3. ACE netCDF File Format Description

A description of the file format of the data is found on the ACE public website on the public dataset page: http://www.ace.uwaterloo.ca/public.html

## 3.4. Public Release (Level 2) Version Details & ReadMe Files

### 3.4.1. ACE-FTS Data Version 2.2, Version 2.2 Ozone Update & Version 2.2 $N_2O_5$ Update ReadMe

ACE version 2.2
May 24th, 2005

Please read the readme files from versions 1.0, 2.0, and 2.1 ACE-FTS processing (located in Section 3.4.3).

The high altitude portion (i.e., above ~90 km) should be improved in this version.

The bug for the output on the retrieval grid (i.e., the tangrid files) has been fixed. One can use either the results on the retrieval grid or the results on the 1-km grid.

The following weak molecules have been added to the processing: HOCl, $H_2O_2$, and $HO_2NO_2$. This is a testing phase for these molecules. As with ClO, averaging results from different occultations may be required.

The retrieval of subsidiary isotopologues begins with this version. Note, however, that there appears to be a problem with HDO retrievals.

A change in the VMR retrieval approach made VMR profiles more susceptible to unphysical oscillations in version 2.0. Care should be taken when comparing to the results for a single ACE occultation. However, comparisons that employ average results from several ACE occultations should not be strongly affected. This problem is not present for any other version of the ACE-FTS processing.

---

ACE version 2.2 $O_3$ update
October 26, 2005

Preliminary validation efforts with ozone suggested that the ACE-FTS retrieval results showed a low bias. The ozone microwindow set consisted of a set in the 1000-1150 $cm^{-1}$ range and a set in 1830-2130 $cm^{-1}$ range. Upon closer inspection, it seems that the spectroscopic information in the two regions is not entirely consistent. The latter microwindow set received a higher weighting in the fitting process (because the SNR was higher in that region) and ended up dominating the fit.

A new set of ozone microwindows was selected, restricting the selection to the 980-1130 $cm^{-1}$ region. The software was upgraded to allow subsidiary isotopes as interferers. Ozone isotopologues 2 and 3 were included as interferers for the updated ozone retrievals.

Tropospheric ozone results showed higher than expected variability. A method used to accelerate the retrieval process runs into trouble where there are significant baseline effects. The speedup was removed for the ozone update.

---

ACE version 2.2 $N_2O_5$ update
September 24, 2010

The $N_2O_5$ update was a bug fix correcting the method the $N_2O_5$ results were written to file. No ReadMe has been prepared specific to the retrieval method of $N_2O_5$ because all relevant information has been supplied in the Version 2.2 ReadMe.

### 3.4.2. ACE-MAESTRO Data Version 1.2 ReadMe

ACE-MAESTRO Data Version 1.2
June 9, 2006

---

*1. A description of the versions*

A version change is caused by these factors: 1) major forward model and/or retrieval algorithm changes; 2) Input data changes such as version changes of the input ACE-FTS retrieved pressure and temperature (p,T) profile data; 3) Changes of the tuning instrument parameters. So far three data products were generated:

Version 1.0: The first MAESTRO data product covers the period from Feb 2004 to May 2005. This version utilized various versions of ACE-FTS retrieved p,T profiles, e.g. versions 1, 2.0, 2.1, 2.2.

Version 1.1: This data set was produced uniformly based on version 2.2 of FTS p,T profiles and covers the period from Feb 2004 to Feb 2006. In the future this version will no longer be processed. Users are encouraged to use version 1.2 instead.

Version 1.2: This data product was also based on uniform version 2.2 of FTS p,T profiles. Comparing to version 1.1 it utilized an optimal set of instrument parameters in time shift, UV spectrometer angle shift and VISIBLE spectrometer angle shift. The three shifts are relative to the ACE-FTS instrument. Version 1.2 is currently at on-going processing stage. Nitrogen dioxide ($NO_2$) and ozone ($O_3$) mixing ratios as well as UV and VISIBLE optical depth are the routine products. Data descriptions are given in section 2 and 3. Section 4 describes the ancillary data such as longitude and latitude information.

---

*2. Mixing ratio data*

Six mixing ratio data products were generated in version 1.2. The files are stored in directories like \2004_02, etc. One directory stores approximately one month of data. Note that one directory of certain month may contain data from other months. The date and time can be determined fully by the file name rather than reflected by the directory name.

The data types can be identified in terms of the fixed sub-strings in the file names.

1) _uno2_: $NO_2$ profile retrieved from the UV spectrometer at the measurement tangent altitudes.
2) _uno2g_: $NO_2$ profile interpolated at the regular tangent height grid from the _uno2_ profile 1).

3) _uo3_: $O_3$ profile retrieved from the UV spectrometer at the measurement tangent altitudes.
4) _uo3g_: $O_3$ profile interpolated at the regular tangent height grid from the _uo3_ profile 3).
5) _vo3_: $O_3$ profile retrieved from the VISIBLE spectrometer at the measurement tangent altitudes.
6) _vo3g_: $O_3$ profile interpolated at the regular tangent height grid from the _vo3_ profile 5).

*2.1 File naming convention of the mixing ratio data*

A file name is composed of following information: orbit number, data type, date and time. For example, "ss2825_uno2_040220_185958_27.dat" reads: "SunSet Orbit ss2825, UV retrieved $NO_2$, measurement starting at 2004/02/20, 18:59:58UTC, using action table 27". Among these items, the action table number is irrelevant to general users.

The file names after Aug. 10, 2005 18:10UTC have an additional 'B' character before the two-digit action table number. This denotes the phase "B" measurement after that time when MAESTRO adopted a new measurement scheme by doubling the sampling rate for the interesting altitude range.

For the SunRise data, the first two letters are "sr".

*2.2 Formats of the mixing ratio data*

Data formats for products at measurement points and interpolated grids are slightly different:

1) At measurement points

Rows 1-10: Ten header lines, indicating the program version and the date. Just skip them.

Follows are 6-column rows:

- Index: Number of the data count.
- Heights: The MAESTRO measurement tangent height estimated from the FTS tangent height. Additional 3 grid points at 654km, 100km and 0km were also included.
- Nitrogen_Dioxide or Ozone: The retrieved Volume Mixing Ratio (VMR) in ppv (parts per volume). The values at 654km, 100km, and 0km were obtained from the first guess.
- Error: The unitless fractional error transformed from instrument noise through the spectral fitting code and profile retrieval. This is essentially the random noise and does not contain the systematic error component.
- Ret: Flag for retrieved with 1, or not retrieved with 0.
- Time: Elapsed seconds in the day.

2) At interpolated regular grid

Rows 1-10: Ten header lines, indicating the program version and the date. Just skip them.

Follows are 5-column rows:

- Index: Number of the data count.
- Heights: A regular grid of the tangent height from 0km to 100km with the interval of 0.5km.
- Nitrogen_Dioxide or Ozone: Logarithmically interpolated Volume Mixing Ratio (VMR) in ppv from the measurement points as given by product 1).
- Error: Unitless fractional error interpolated from the measurement points.
- Retrieved?: Flag for retrieved with 1, or not retrieved with 0.

---

*3. The optical depth data*

The optical depth data are produced as a routine product. They are stored in directories od_h\2004_02\ ... on monthly basis. Like the mixing ratio data the date and time can be determined fully by the file name.

*3.1 The file naming convention of the optical depth data*

The optical depth data have two files for each measurement. One is for UV, the other for VISIBLE. The naming convention is similar to the mixing ratio files.

For example, "ss2826_odu_040220_185958_27.dat" reads: "Sunset Orbit 2826, Optical Depth for UV, measurement starts at 2004/02/20 18:59:58UTC, using action table 27".

The file names after Aug. 10, 2005 18:10UTC have an extra 'B' character before the two-digit action table number. This denotes the phase "B" measurement after that time when MAESTRO adopted a new sampling scheme.

For the corresponding VISIBLE optical depth data, the sub-string "odu" is replaced by "odv".

For the SunRise data, the first two letters are "sr".

*3.2 Optical Depth data format*

Both UV and VISIBLE optical depth data have the same format. The structure is as follows:

i) Rows 1-2: Two header lines of the file, just skip them.

ii) Row 3: One header line for one spectrum measurement. In this line, three parameters after "TIME:" are important. They are date (yymmdd), time in UTC (hhmmss), elapsed kilo-seconds of the day. For example, in "ss2826_odu_040220_185958_27.dat", the third row contains "TIME: 040220 190042.080 68.442080", meaning "date at 2004/02/20, time at 19:00:42.08UTC, which is equivalent to the elapsed 68.442080 ksec in kilo-seconds".

iii) Row 4: The tangent height in km at the time given in Row 3. Any missing altitude is filled with a default value of 999.9.

iv) Rows 5 - 1029: The 1024 lines represent 1024 pixels of the optical depth. Each row is given by two columns: the first is the estimated wavelength in nm, the second the optical depth (unitless). The data gaps are filled with either infinite number of "1.#INF0e+000" or a Non-A-Number of "-1.#IND0e+000".

v) Repeat ii) - iv) for N times.

*4. Ancillary data*

Ancillary data are those additional data associated with the measurement such as geolocation data. The linkage of the profile data or optical depth data with the ancillary data is through the common orbit number. The orbit number is the common key for linking all different types of data in ACE database.

*4.1 Geolocation data*

Two files "SunriseTable.txt" and "SunsetTable.txt" are lookup tables of partial geolocation information for each occultation. Each file contains six columns. They are:

- Orbit number
- Date
- Time in UTC at 30km tangent height
- latitude at 30km tangent height
- longitude at 30km tangent height
- beta angle

---

*5. Reference*

The background of the instrument and the retrieval can be found in:

McElroy C.T. (1995), A spectroradiometer for the measurement of direct and scattered solar spectral irradiance from on-board the NASA ER-2 high altitude research aircraft, Geophys. Res. Lett., 22, 1361-1364.

McElroy C.T., C. Midwinter, D.V. Barton, and R.B. Hall (1995), A comparison of J-values estimated by the composition and photodissociative flux measurement with model calculation, Geophys. Res. Lett., 22, 1365-1368.

## 3.4.3. Historical ACE-FTS ReadMe Files

### 3.4.3.1. ACE-FTS Data Version 1.0 ReadMe

ACE version 1.0
September 11, 2004

Some issues to be aware of with the ACE data

In the vmr results, an entry of -999 indicates that no retrieval was performed at that altitude. At high altitudes, above the highest measurement used in the analysis for a given molecule, I include a VERY rough estimate of the molecule's vmr (it is a constant times the a priori value, with the same constant used for all altitudes above the highest analysed measurement). These data are flagged by the uncertainties being set to -888. Do not trust these results too far above the highest analyzed measurement.

Pressure and temperature values were retrieved down to no lower than 12 km (the columun labelled T_Fit indicates whether temperature was retrieved at that altitude: T

for True and F for False). Below 12 km, temperature and pressure were fixed to data from the Canadian Meteorological Center.

High altitude results (above about 95 km) should be viewed with skepticism. The temperature profiles above this altitude require further work.

No provision was made for indentifying occultations with significant ice contamination on the FTS detectors. Therefore, some occultations (particularly earlier ones) could experience a deterioration of results at low altitudes, some molecules worse than others.

Uncertainties provided for the vmr results are statistical errors from the fitting process (1-sigma), and do not include systematic contributions. A more detailed error budget will be determined later.

The molecule NO sometimes has extremely low absorption through the mesosphere (increasing for both higher and lower altitudes). For such occultations, the retrieved NO profile through the mesosphere will look quite ugly. The results are to be ignored when this happens.

For occultations that cut out above 10-17 km (due to clouds), the bottom-most measurement often gives results that are clearly out (presumably from the clouds affecting the measurement just before the suntracker loses lock). Simply ignore the bottom point if it looks inconsistent.

For molecules with significant interferences (e.g., $N_2O_5$ and $SF_6$), the vmr for the highest analyzed measurement is sometimes suspiciously high. I am investigating the cause of this. If you see a sharp increase in the highest retrieved points, don't trust it.

### 3.4.3.2. ACE-FTS Data Version 2.0 ReadMe

ACE version 2.0
January 20, 2005 - updated May 24, 2005

Please read the ACE_readme.txt file from ACE-FTS version 1.0 processing. The setup of the output files is the same as for version 1.0, although there are more molecules. Recall the papers available for background information:

> Bernath, P. F., et al. (2005), **Atmospheric Chemistry Experiment (ACE): Mission overview**, Geophys. Res. Lett., 32, L15S01, doi:10.1029/2005GL022386
>
> Boone, Christopher D., et al. (2005), **Retrievals for the atmospheric chemistry experiment Fourier-transform spectrometer**, Applied Optics, Vol. 44, No. 33, 7218-7231

Pre-prints of the papers can be found on the following Web site: http://www.ace.uwaterloo.ca/publications.html

In the T_fit column, 1 and 0 are used to replace T and F, respectively, from the version 1.0 output format.

Version 2.0 output files give results on both the standard 1-km grid and on the measurement grid.

For version 2.0, problems encountered when measurement spacings were less than 1 km (the altitude grid spacing) have been addressed.

A slightly improved approach is used for interpolating onto the 1-km grid for forward model calculations. In version 1.0, you could get a (maximum 0.5 km) extrapolation that would serve to slightly enhance unphysical oscillations in the results (when they were present).

For pressure/temperature retrievals below 25 km, an empirical expression with four parameters is used for pressure retrievals (instead of using a parameter for each measurement).

For P/T processing, a bug was fixed whereby during retrievals below the "crossover", P and T were fixed to the results of the retrieval above the crossover (rather than being fixed to the a priori P and T).

The software was converted to use exclusively HITRAN molecule numbering (rather than using ATMOS molecule numbering with the HITRAN 2004 linelist). A mismatch between the assumed molecule numbering and the molecule numbers in the linelist caused some issues in the troposphere (because of "phantom interferences").

The ability to retrieve subsidiary isotopologues was implemented in the software. As of January 20th, 2005, the isotopologues were not being retrieved, awaiting completion of microwindow selection. A second pass with the software will fill in the isotopologue results. Note that HDO, which was included in the regular output files for version 1.0, will now be in a separate file with all of the other subsidiary isotopologues.

Columns in the output files exist for some weak absorbers ($HO_2NO_2$, $H_2O_2$, HOCl, $H_2CO$, and HCOOH) that are not being retrieved. They will also be retrieved on a second pass of processing, once I am comfortable with the ability to retrieve them reliably.

With a broader sample of atmospheric conditions available for evaluating microwindows, the microwindow selection was revised to avoid instances of saturation. More microwindows were added at low altitudes for several molecules to improve tropospheric results.

*$H_2O$*: Microwindows changed to (1) avoid saturation experienced for some occultations, (2) avoid the 3200 $cm^{-1}$ region (which was strongly impacted by detector contamination), (3) improve tropospheric retrievals, and (4) have fewer interferences in the multiple molecule retrievals

*$O_3$*: The upper altitude limit of the retrieval range was increased to 95 km. Microwindow selection was redone to avoid significant interference from the

668 and 686 isotopologues and to get more microwindows in the troposphere. More windows were also added in the vicinity of the $O_3$ concentration peak.

*$N_2O$*: More microwindows at lower altitudes, particularly for the troposphere.

*CO*: Microwindows were adjusted improve results at low altitudes, particularly for the troposphere.

*$NO_2$*: The upper altitude limit was increased, mostly to capture the enhanced high altitude $NO_x$ observed during February, 2004.

*HCl*: More microwindows were added, particularly at high altitudes.

*$COF_2$*: Microwindows were adjusted to avoid residual solar features. More lines were included in the retrieval.

*$SF_6$*: The upper altitude limit was lowered to improve retrievals.

The following molecules have been added for version 2.0 that were not retrieved in version 1.0: OCS, HCN, $CF_4$, $CH_3Cl$, $C_2H_2$, $C_2H_6$, and $N_2$

**Addendum (May 24, 2005):**
A change in the VMR retrieval approach made VMR profiles more susceptible to unphysical oscillations in version 2.0. Care should be taken when comparing to the results for a single ACE occultation. However, comparisons that employ average results from several ACE occultations should not be strongly affected. This problem is not present for any other version of the ACE-FTS processing.

### 3.4.3.3. ACE-FTS Data Version 2.1 ReadMe

ACE version 2.1
May 24th, 2005

Please read the readme files from versions 1.0 and 2.0 ACE-FTS processing.

Version 2.1 processing was only performed on a subset of the measured occultations, mostly concentrating on the Arctic measurements during January-March 2005. There was significant ice contamination on the detectors during this time period. Results for some molecules are expected to be noisier than usual, particularly HCN. $ClONO_2$ below 18 km could also exhibit increased noise.

The results on the retrieval grid (i.e., the "tangrid" files) did not always output properly. Use the results on the 1-km grid. Note that the same issue exists for version 2.0.

ClO was added to the retrievals. This is a very weak absorber, and so it may be better to average results for several occultations with similar conditions rather than considering the results from a single occultation. There only appears to be significant ClO present during the Arctic spring occultations in this data set.

$C_2H_2$ does not appear to be processing properly.

# References


Bernath, Peter (2006), *Atmospheric Chemistry Experiment (ACE): Analytical Chemistry from Orbit*, Trends in Analytical Chemistry, Vol. 25, No. 7, pp. 647-654.

Bernath, P. F., C.T. McElroy, M.C. Abrams, C.D. Boone, M. Butler, C. Camy-Peyret, M. Carleer, C. Clerbaux, P.F. Coheur, R. Colin, P. DeCola, M. DeMazière, J.R. Drummond, D. Dufour, W.F.J. Evans, H. Fast, D. Fussen, K. Gilbert, D.E. Jennings, E.J. Llewellyn, R.P. Lowe, E. Mahieu, J.C. McConnell, M. McHugh, S.D. McLeod, R. Michaud, C. Midwinter, R. Nassar, F. Nichitiu, C. Nowlan, C.P. Rinsland, Y.J. Rochon, N. Rowlands, K. Semeniuk, P. Simon, R. Skelton, J.J. Sloan, M.-A. Soucy, K. Strong, P. Tremblay, D. Turnbull, K.A. Walker, I. Walkty, D.A. Wardle, V. Wehrle, R. Zander, and J. Zou (2005), *Atmospheric Chemistry Experiment (ACE): Mission overview*, Geophys. Res. Lett., 32, L15S01, doi:10.1029/2005GL022386.

Boone, Christopher D., Ray Nassar, Kaley A. Walker, Yves Rochon, Sean D. McLeod, Curtis P. Rinsland, and Peter F. Bernath (2005), *Retrievals for the atmospheric chemistry experiment Fourier-transform spectrometer*, Applied Optics, Vol. 44, No. 33, 7218-7231.

Burrows, J.P., M. Weber, M. Buchwitz, V. Rozanov, A. Ladstätter-Weißenmayer, A. Richter, R. DeBeek, R. Hoogen, K. Bramstedt, K.-U. Eichmann, M. Eisinger, D. Perner (1999), *The Global Ozone Monitoring Experiment (GOME): Mission Concept and First Scientific Results*, J. Atmos. Sci., 56, 151-175.

Carleer, M.R., C.D. Boone, K.A. Walker, P.F. Bernath, K. Strong, R.J. Sica, C.E. Randall, H. Vömel, J. Kar, M. Höpfner, M. Milz, T. von Clarmann, R. Kivi, J. Valverde-Canossa, C.E. Sioris, M.R.M. Izawa, E. Dupuy, C.T. McElroy, J.R. Drummond, C.R. Nowlan, J. Zou, F. Nichitiu, S. Lossow, J. Urban, D. Murtagh, and D.G. Dufour (2008), *Validation of water vapour profiles from the Atmospheric Chemistry Experiment (ACE)*, Atmos. Chem. Phys. Discuss., 8, 4499-4559.

Clerbaux, C., George, M., Turquety, S., Walker, K.A., Barret, B., Bernath, P., Boone, C., Borsdorff, T., Cammas, J.P., Catoire, V., Coffey, M., Coheur, P.-F., Deeter, M., De Mazière, M., Drummond, J., Duchatelet, P., Dupuy, E., de Zafra, R., Eddounia, F., Edwards, D.P., Emmons, L., Funke, B., Gille, J., Griffith, D.W.T., Hannigan, J., Hase, F., Höpfner, M., Jones, N., Kagawa, A., Kasai, Y., Kramer, I., Le Flochmoën, E., Livesey, N.J., López-Puertas, M., Luo, M., Mahieu, E., Murtagh, D., Nédélec, P., Pazmino, A., Pumphrey, H., Ricaud, P., Rinsland, C.P., Robert, C., Schneider, M., Senten, C., Stiller, G., Strandberg, A., Strong, K., Sussmann, R., Thouret, V., Urban, J., and Wiacek, A. (2008), *CO measurements from the ACE-FTS satellite instrument: data analysis and validation using ground-based, airborne and spaceborne observations*, Atmos. Chem. Phys., 8, 2569-2594.

De Mazière, M., C. Vigouroux, P. F. Bernath, P. Baron, T. Blumenstock, C. Boone, C. Brogniez, V. Catoire, M. Coffey, P. Duchatelet, D. Griffith, J. Hannigan, Y. Kasai, I. Kramer, N. Jones, E. Mahieu, G. L. Manney, C. Piccolo, C. Randall, C. Robert, C. Senten, K. Strong, J. Taylor, C. Tétard, K. A. Walker and S. Wood (2008), *Validation of ACE-FTS v2.2 methane profiles from the upper troposphere to lower mesosphere*, Atmos. Chem. Phys., 8, 2421-2435.

Dupuy, E., K.A. Walker, J. Kar, C.D. Boone, C.T. McElroy, P.F. Bernath, J.R. Drummond, R. Skelton, S.D. McLeod, R.C. Hughes, C.R. Nowlan, D.G. Dufour, J. Zou, F. Nichitiu, K. Strong, P. Baron, R.M. Bevilacqua, T. Blumenstock, G.E. Bodeker, T. Borsdorff, A.E. Bourassa, H. Bovensmann, I.S. Boyd, A. Bracher, C. Brogniez, J.P. Burrows, V. Catoire, S. Ceccherini, S. Chabrillat, T. Christensen, M.T. Coffey, U. Cortesi, J. Davies, C. De Clercq, D.A. Degenstein, M. De Mazière, P. Demoulin, J. Dodion, B. Firanski, H. Fischer, G. Forbes, L. Froidevaux, D. Fussen, P. Gerard, S. Godin-Beekmann, F. Goutail, J. Granville, D. Griffith, C.S. Haley, J.W. Hannigan, M. Höpfner, J.J. Jin, A. Jones, N.B. Jones, K. Jucks, A. Kagawa, Y. Kasai, T.E. Kerzenmacher, A. Kleinböhl, A.R. Klekociuk, I. Kramer, H. K¨llmann, J. Kuttippurath, E. Kyrölä, J.-C. Lambert, N.J. Livesey, E.J. Llewellyn, N.D. Lloyd, E. Mahieu, G.L. Manney, B.T. Marshall, J.C. McConnell, M.P. McCormick, I.S. McDermid, M. McHugh, C.A. McLinden, J. Mellqvist, K. Mizutani, Y. Murayama, D.P. Murtagh, H. Oelhaf, A. Parrish, S.V. Petelina, C. Piccolo, J.-P. Pommereau, C.E. Randall, C. Robert, C. Roth, M. Schneider, C. Senten, T. Steck, A. Strandberg, K.B. Strawbridge, R. Sussmann, D.P.J. Swart, D.W. Tarasick, J.R. Taylor, C. Tétard, L.W. Thomason, A.M. Thompson, M.B. Tully, J. Urban, F. Vanhellemont, C. Vigouroux, T. von Clarmann, P. von der Gathen, C. von Savigny, J.W. Waters, J.C. Witte, M. Wolff, and J.M. Zawodny (2009), *Validation of ozone measurements from the Atmospheric Chemistry Experiment (ACE)*, Atmos. Chem. Phys., 9, 287-343.

Gilbert, K.L., D.N. Turnbull, K.A. Walker, C.D. Boone, S.D. McLeod, M. Butler, R. Skelton, P.F. Bernath, F. Châteauneuf and M.-A. Soucy (2007), *The onboard imagers for the Canadian ACE SCISAT-1 mission*, J. Geophys. Res., Vol. 112, D12207, doi:10.1029/2006JD007714.

Kent, G.S., D. M. Winker, M. T. Osborn, K. M. Skeens (1993), *A Model for the Separation of Cloud and Aerosol in SAGE II Occultation Data*, J. Geophys. Res., 98(D11), 20725-20735.

Kerzenmacher, T., M.A. Wolff, K. Strong, E. Dupuy, K.A. Walker, L.K. Amekudzi, R.L. Batchelor, P.F. Bernath, G. Berthet, T. Blumenstock, C.D. Boone, K. Bramstedt, C. Brogniez, S. Brohede, J.P. Burrows, V. Catoire, J. Dodion, J.R. Drummond, D.G. Dufour, B. Funke, D. Fussen, F. Goutail, D.W.T. Griffith, C.S. Haley, F. Hendrick, M. Höpfner, N. Huret, N. Jones, J. Kar, I. Kramer, E.J. Llewellyn, M. López-Puertas, G. Manney, C.T. McElroy, C.A. McLinden, S. Melo, S. Mikuteit, D. Murtagh, F. Nichitiu, J. Notholt, C. Nowlan, C. Piccolo, J.-P. Pommereau, C. Randall, P. Raspollini, M. Ridolfi, A. Richter, M. Schneider, O. Schrems, M. Silicani, G.P. Stiller, J. Taylor, C. Tétard, M. Toohey, F. Vanhellemont, T. Warneke, J.M. Zawodny, and J. Zou (2008), *Validation of $NO_2$ and NO from the Atmospheric Chemistry Experiment (ACE)*, Atmos. Chem. Phys., 8, 5801-5841.

Mahieu, E., P. Duchatelet, P. Demoulin, K.A. Walker, E. Dupuy, L. Froidevaux, C. Randall, V. Catoire, K. Strong, C.D. Boone, P.F. Bernath, J.-F. Blavier, T. Blumenstock, M. Coffey, M. De Mazière, D. Griffith, J. Hannigan, F. Hase, N. Jones, K. W. Jucks, A. Kagawa, Y. Kasai, Y. Mebarki, S. Mikuteit, R. Nassar, J. Notholt, C.P. Rinsland, C. Robert, O. Schrems, C. Senten, D. Smale, J. Taylor, C. Tétard, G.C. Toon, T. Warneke, S.W. Wood, R. Zander, and C. Servais (2008), *Validation of ACE-FTS v2.2 Measurements of HCl, HF, $CCl_3F$, and $CCl_2F_2$ using space-, balloon- and ground-based instrument observations*, Atmos. Chem. Phys., 8, 6199-6221.

McElroy C.T. (1995), *A spectroradiometer for the measurement of direct and scattered solar spectral irradiance from on-board the NASA ER-2 high altitude research aircraft*, Geophys. Res. Lett., 22, 1361-1364.

McElroy C.T., C. Midwinter, D.V. Barton, and R.B. Hall (1995), *A comparison of J-values estimated by the composition and photodissociative flux measurement with model calculation*, Geophys. Res. Lett., 22, 1365-1368.

McElroy, C. Thomas, Caroline R. Nowlan, James R. Drummond, Peter F. Bernath, David V. Barton, Denis G. Dufour, Clive Midwinter, Robert B. Hall, Akira Ogyu, Aaron Ullberg, David I. Wardle, Jay Kar, Jason Zou, Florian Nichitiu, Chris D. Boone, Kaley A. Walker and Neil Rowlands (2007), *The ACE-MAESTRO Instrument on SCISAT: description, performance and preliminary results*, Applied Optics, Vol. 46, No. 20, 4341-4356.

Sica, R.J., M.R.M. Izawa, K.A. Walker, C. Boone, S.V. Petelina, P.S. Argall, P. Bernath, G. B. Burns, V. Catoire, R.L. Collins, W.H. Daffer, C. De Clercq, Z.Y. Fan, B.J. Firanski, W.J.R. French, P. Gerard, M. Gerding, J. Granville, J.L. Innis, P. Keckhut, T. Kerzenmacher, A.R. Klekociuk, E. Kyrö, J.C. Lambert, E.J. Llewellyn, G.L. Manney, I.S. McDermid, K. Mizutani, Y. Murayama, C. Piccolo, P. Raspollini, M. Ridolfi, C. Robert, W. Steinbrecht, K.B. Strawbridge, K. Strong, R. Stübi and B. Thurairajah (2008), *Validation of the Atmospheric Chemistry Experiment (ACE) version 2.2 temperature using ground based and space-borne measurements*, Atmos. Chem. Phys., 8, 35-62.

Strong, K., M.A. Wolff, T.E. Kerzenmacher, K.A. Walker, P.F. Bernath, T. Blumenstock, C. Boone, V. Catoire, M. Coffey, M. De Mazière, P. Demoulin, P. Duchatelet, E. Dupuy, J. Hannigan, M. Höpfner, N. Glatthor, D.W. T. Griffith, J.J. Jin, N. Jones, K. Jucks, H. Kuellmann, J. Kuttippurath, A. Lambert, E. Mahieu, J.C. McConnell, J. Mellqvist, S. Mikuteit, D.P. Murtagh, J. Notholt, C. Piccolo, P. Raspollini, M. Ridolfii, C. Robert, M. Schneider, O. Schrems, K. Semeniuk, C. Senten, G.P. Stiller, A. Strandberg, J. Taylor, C. Tétard, M. Toohey, J. Urban, T. Warneke, and S. Wood (2008), *Validation of ACE-FTS $N_2O$ measurements*, Atmos. Chem. Phys., 8, 4759-4786.

Vanhellemont, F., C. Tetard, A. Bourassa, M. Fromm, J. Dodion, D. Fussen, C. Brogniez, K.L. Gilbert, D.N. Turnbull, P. Bernath, C. Boone and K.A. Walker (2008), *Validation of 525 nm and 1020 nm aerosol extinction profiles derived from ACE imager data: comparisons with GOMOS, SAGE II, SAGE III, POAM III, and OSIRIS*, Atmos. Chem. Phys., 8, 2027-2037.

Wolff, M.A., T. Kerzenmacher, K. Strong, K.A. Walker, M. Toohey, E. Dupuy, P.F. Bernath, C.D. Boone, S. Brohede, V. Catoire, T. von Clarmann, M. Coffey, W.H. Daffer, M. De Mazière, P. Duchatelet, N. Glatthor, D.W.T. Griffith, J. Hannigan, F. Hase, M. Höpfner, N. Huret, N. Jones, K. Jucks, A. Kagawa, Y. Kasai, I. Kramer, H. Küllmann, J. Kuttippurath, E. Mahieu, G. Manney, C. McLinden, Y. Mébarki, S. Mikuteit, D. Murtagh, C. Piccolo, P. Raspollini, M. Ridolfi, R. Ruhnke, M. Santee, C. Senten, D. Smale, C. Tétard, J. Urban, and S. Wood (2008), *Validation of $HNO_3$, $ClONO_2$, and $N_2O_5$ from the Atmospheric Chemistry Experiment Fourier Transform Spectrometer (ACE-FTS)*, Atmos. Chem. Phys., 8, 3529-3562.

# Appendix A: Glossary

**Beta Angle:** the angle between the orbital plane of the satellite and the Earth-Sun vector. See Section 2.7

**Measurement:** a single scan of the FTS instrument. This action produces a single spectrum

**Occultation:** a successive series of measurements by the FTS that produces a profile of the atmosphere

**Profile:** a "side" view of the atmosphere. In graphing, the Y-axis would be increasing altitude above the Earth's surface

**SCISAT:** the name of the satellite which contains the ACE-FTS, ACE-MAESTRO and ACE-Imagers

**Sunrise:** the process of going from being in eclipse (shadow, no sunlight) to being in sunlight.

**Sunset:** the process of going from being in sunlight to being in eclipse (shadow, no sunlight)

**Tangent Point:** the shortest distance between the Earth's surface and the line between the satellite and the Sun. In Figure 3 the Tangent Point is the point of closest approach between the Earth's surface and Measurement n (1, 2, 3, etc.). This value is only relevant during a measurement

**Vertical Spacing**: the vertical distance between successive measurements

# Appendix B: Acronym List

**ACE:** Atmospheric Chemistry Experiment

**ATMOS:** Atmospheric Trace MOlecule Spectroscopy

**FOV:** Field Of View

**FTS:** Fourier Transform Spectrometer

**GOME:** Global Ozone Monitoring Experiment

**GOMOS:** Global Ozone Monitoring of Occultation of Stars

**MAESTRO:** Measurement of Aerosol Extinction in the Stratosphere and Troposphere by Occultation

**NIR:** Near-InfraRed

**OSIRIS:** Optical Spectrograph and InfraRed Imaging System

**POAM:** Polar Ozone and Aerosol Measurement

**SAGE:** Stratospheric Aerosol and Gas Experiment

**SNR:** Signal-to-Noise Ratio

**VMR**: Volume Mixing Ratio

**UV:** UltraViolet

# Appendix C: Microwindow List

Microwindow sets used for the ACE-FTS version 2.2 volume mixing ratio (VMR) retrievals are presented. Also reported are the molecules explicitly included as interferers in the retrieval of the target molecule. The VMR profiles for these interferences are fitted simultaneously with the target VMR profile. For some molecules, additional interferences exist that are not explicitly retrieved, in which case the VMR profile for the interferers are fixed to the results of previous retrievals.

Some molecules (such as $C_2H_6$) have an upper altitude limit that varies with latitude. The lower value listed in the table corresponds to the upper altitude limit at the poles, while the higher value corresponds to the upper altitude limit at the equator.

The $O_3$ microwindows listed here are for the "version 2.2 $O_3$ update" set of results. The microwindows used in the normal version 2.2 processing are not included. Note that there was no change in microwindows for the HDO update. Changes for this isotopologue were in the processing software, not the microwindow set.

Some microwindow sets include windows that do not contain information on the target molecule, but instead are meant to improve the results for the interferences, particularly for cases where the spectral features from the interferences in the main microwindow set are relatively weak.

The weighting factor used for the least squares process varied with wavenumber because the signal-to-noise ratio (SNR) in the spectrum varies with wavenumber. The table below details the assumed SNR used to calculate the fitting weights (the weighting goes as the square of the SNR). Note that the actual SNR performance of the instrument is typically underestimated by these effective values. The purpose of these values is to apply a relative fitting weight for microwindows from different wavenumber ranges for a given molecule.

**Table 4: Signal-to-Noise Weighting of Wavenumber Ranges**

| Range ($cm^{-1}$) | Effective SNR |
|---|---|
| < 800 | 50 |
| 800 – 900 | 75 |
| 900 – 1000 | 100 |
| 1000 – 1850 | 175 |
| 1850 – 2500 | 200 |
| 2500 – 2750 | 125 |
| 2750 – 3900 | 100 |
| 3900 – 4100 | 70 |
| 4100 – 4200 | 50 |
| > 4200 | 35 |

**Table 5: Microwindow list for Pressure/Temperature**

| Center Wavenumber ($cm^{-1}$) | Microwindow Width ($cm^{-1}$) | Lower Altitude (km) | Upper Altitude (km) |
|---|---|---|---|
| 932.96 | 0.30 | 12 | 20 |
| 934.90 | 0.30 | 12 | 20 |
| 936.80 | 0.35 | 12 | 20 |
| 1890.34 | 0.24 | 17 | 47 |
| 1899.17 | 0.30 | 25 | 58 |
| 1902.05 | 0.30 | 30 | 60 |
| 1905.09 | 0.30 | 27 | 63 |
| 1906.48 | 0.30 | 30 | 65 |
| 1911.02 | 0.35 | 35 | 68 |
| 1912.52 | 0.35 | 45 | 68 |
| 1914.11 | 0.30 | 40 | 70 |
| 1915.48 | 0.35 | 39 | 70 |
| 1917.06 | 0.35 | 30 | 70 |
| 1918.49 | 0.30 | 38 | 70 |
| 1920.11 | 0.35 | 30 | 70 |
| 1924.71 | 0.35 | 35 | 65 |
| 1927.70 | 0.30 | 27 | 61 |
| 1929.35 | 0.35 | 21 | 56 |
| 1933.90 | 0.40 | 24 | 60 |
| 1934.62 | 0.30 | 20 | 54 |
| 1935.23 | 0.30 | 15 | 50 |
| 1936.44 | 0.30 | 23 | 50 |
| 1941.12 | 0.35 | 15 | 42 |
| 1950.68 | 0.30 | 12 | 43 |
| 1955.49 | 0.30 | 20 | 50 |
| 1963.59 | 0.30 | 20 | 50 |
| 1968.63 | 0.30 | 12 | 50 |
| 1970.10 | 0.30 | 15 | 48 |
| 1975.15 | 0.20 | 12 | 40 |
| 2042.93 | 0.30 | 48 | 68 |
| 2044.50 | 0.30 | 50 | 70 |
| 2045.97 | 0.30 | 53 | 73 |
| 2047.53 | 0.40 | 55 | 73 |
| 2049.05 | 0.40 | 53 | 75 |
| 2050.55 | 0.40 | 55 | 78 |
| 2052.10 | 0.30 | 50 | 79 |
| 2053.66 | 0.30 | 55 | 80 |
| 2055.11 | 0.35 | 60 | 80 |
| 2056.72 | 0.30 | 55 | 85 |
| 2058.24 | 0.40 | 55 | 85 |
| 2061.33 | 0.35 | 60 | 85 |
| 2062.87 | 0.35 | 60 | 85 |
| 2066.03 | 0.35 | 60 | 85 |
| 2067.52 | 0.35 | 60 | 83 |

**Table 5: Microwindow list for Pressure/Temperature (continued)**

| Center Wavenumber ($cm^{-1}$) | Microwindow Width ($cm^{-1}$) | Lower Altitude (km) | Upper Altitude (km) |
|---|---|---|---|
| 2070.65 | 0.40 | 62 | 80 |
| 2072.23 | 0.30 | 57 | 80 |
| 2277.43 | 0.30 | 42 | 68 |
| 2293.77 | 0.55 | 78 | 94 |
| 2296.05 | 0.26 | 80 | 100 |
| 2300.40 | 0.30 | 82 | 115 |
| 2306.85 | 0.30 | 90 | 125 |
| 2313.10 | 0.35 | 100 | 130 |
| 2319.14 | 0.26 | 105 | 130 |
| 2323.15 | 0.30 | 105 | 130 |
| 2332.37 | 0.30 | 105 | 130 |
| 2354.37 | 0.26 | 105 | 130 |
| 2361.45 | 0.30 | 105 | 130 |
| 2364.10 | 0.30 | 105 | 130 |
| 2366.63 | 0.30 | 105 | 130 |
| 2367.88 | 0.30 | 105 | 130 |
| 2369.10 | 0.30 | 105 | 130 |
| 2370.27 | 0.35 | 105 | 130 |
| 2371.43 | 0.30 | 105 | 130 |
| 2372.56 | 0.30 | 105 | 130 |
| 2373.67 | 0.35 | 105 | 130 |
| 2374.75 | 0.40 | 100 | 130 |
| 2375.80 | 0.35 | 100 | 130 |
| 2376.84 | 0.35 | 95 | 130 |
| 2377.85 | 0.35 | 95 | 125 |
| 2378.83 | 0.35 | 93 | 123 |
| 2379.78 | 0.35 | 90 | 120 |
| 2380.72 | 0.35 | 85 | 115 |
| 2381.62 | 0.35 | 85 | 115 |
| 2382.48 | 0.40 | 82 | 115 |
| 2383.36 | 0.35 | 82 | 115 |
| 2384.19 | 0.35 | 79 | 115 |
| 2385.02 | 0.40 | 75 | 95 |
| 2385.79 | 0.35 | 73 | 90 |
| 2386.51 | 0.35 | 70 | 86 |
| 2387.26 | 0.35 | 65 | 83 |
| 2387.96 | 0.35 | 60 | 80 |
| 2388.64 | 0.35 | 55 | 77 |
| 2389.29 | 0.35 | 50 | 71 |
| 2389.92 | 0.30 | 35 | 68 |
| 2390.52 | 0.35 | 33 | 65 |
| 2391.13 | 0.30 | 25 | 62 |
| 2391.70 | 0.30 | 22 | 60 |
| 2392.10 | 0.30 | 20 | 55 |
| 2392.62 | 0.30 | 20 | 50 |
| 2393.06 | 0.30 | 25 | 50 |

**Table 5: Microwindow list for Pressure/Temperature (continued)**

| Center Wavenumber ($cm^{-1}$) | Microwindow Width ($cm^{-1}$) | Lower Altitude (km) | Upper Altitude (km) |
|---|---|---|---|
| 2408.77 | 0.20 | 15 | 46 |
| 2412.47 | 0.30 | 15 | 46 |
| 2421.19 | 0.30 | 15 | 46 |
| 2422.88 | 0.30 | 15 | 46 |
| 2437.60 | 0.22 | 15 | 46 |
| 2439.00 | 0.30 | 15 | 46 |
| 2440.28 | 0.20 | 17 | 46 |
| 2444.27 | 0.24 | 15 | 46 |
| 2447.89 | 0.26 | 15 | 43 |
| 3301.52 | 0.30 | 12 | 25 |
| 3304.67 | 0.30 | 12 | 30 |
| 3306.29 | 0.30 | 12 | 31 |
| 3330.00 | 0.30 | 12 | 22 |
| 3377.06 | 0.26 | 12 | 30 |
| 3378.64 | 0.26 | 12 | 25 |
| 3380.03 | 0.30 | 12 | 20 |

**Table 6: Microwindow list for $H_2O$**

| Center Wavenumber ($cm^{-1}$) | Microwindow Width ($cm^{-1}$) | Lower Altitude (km) | Upper Altitude (km) |
|---|---|---|---|
| 953.43 | 0.45 | 5 | 9 |
| 955.25 | 0.50 | 5 | 8 |
| 971.34 | 0.35 | 5 | 12 |
| 973.99 | 0.40 | 5 | 12 |
| 1362.60 | 0.30 | 50 | 70 |
| 1375.06 | 0.35 | 40 | 75 |
| 1379.56 | 0.30 | 30 | 55 |
| 1388.52 | 0.28 | 15 | 45 |
| 1428.21 | 0.30 | 20 | 55 |
| 1429.95 | 0.35 | 44 | 70 |
| 1456.84 | 0.30 | 50 | 84 |
| 1496.25 | 0.35 | 50 | 84 |
| 1505.57 | 0.35 | 54 | 90 |
| 1507.06 | 0.35 | 53 | 90 |
| 1539.06 | 0.35 | 70 | 90 |
| 1540.30 | 0.35 | 60 | 86 |
| 1553.00 | 0.35 | 15 | 40 |
| 1558.53 | 0.35 | 55 | 90 |
| 1560.26 | 0.35 | 54 | 86 |
| 1562.64 | 0.30 | 15 | 35 |
| 1568.94 | 0.35 | 44 | 75 |

**Table 6: Microwindow list for $H_2O$ (continued)**

| Center Wavenumber ($cm^{-1}$) | Microwindow Width ($cm^{-1}$) | Lower Altitude (km) | Upper Altitude (km) |
|---|---|---|---|
| 1576.19 | 0.35 | 55 | 90 |
| 1616.71 | 0.35 | 75 | 90 |
| 1623.56 | 0.35 | 50 | 82 |
| 1635.65 | 0.35 | 54 | 86 |
| 1652.40 | 0.40 | 75 | 90 |
| 1653.23 | 0.30 | 60 | 90 |
| 1662.81 | 0.35 | 50 | 84 |
| 1668.28 | 0.35 | 40 | 75 |
| 1669.30 | 0.50 | 65 | 83 |
| 1672.42 | 0.30 | 30 | 65 |
| 1684.84 | 0.35 | 55 | 90 |
| 1695.93 | 0.35 | 65 | 90 |
| 1699.94 | 0.35 | 55 | 90 |
| 1734.53 | 0.45 | 55 | 85 |
| 1739.84 | 0.35 | 60 | 80 |
| 1752.75 | 0.30 | 30 | 60 |
| 1767.04 | 0.40 | 15 | 45 |
| 1770.91 | 0.35 | 40 | 60 |
| 1788.36 | 0.30 | 15 | 50 |
| 1788.66 | 0.30 | 15 | 35 |
| 1805.13 | 0.30 | 40 | 60 |
| 1837.43 | 0.30 | 25 | 45 |
| 1856.20 | 0.40 | 15 | 40 |
| 1904.36 | 0.35 | 35 | 55 |
| 1940.24 | 0.30 | 8 | 15 |
| 1945.34 | 0.35 | 35 | 60 |
| 1946.31 | 0.30 | 35 | 60 |
| 1950.10 | 0.35 | 7 | 15 |
| 1951.11 | 0.18 | 12 | 30 |
| 1954.98 | 0.25 | 23 | 55 |
| 1956.33 | 0.30 | 17 | 40 |
| 1959.58 | 0.40 | 7 | 30 |
| 1961.15 | 0.30 | 20 | 55 |
| 1966.26 | 0.35 | 33 | 60 |
| 1969.82 | 0.26 | 7 | 9 |
| 1976.20 | 0.25 | 15 | 45 |
| 1987.34 | 0.30 | 12 | 20 |
| 1989.96 | 0.26 | 8 | 15 |
| 1999.92 | 0.30 | 7 | 12 |

**Table 7: Interfering molecule(s) for $H_2O$**

| Molecule | Upper Altitude Limit (km) |
|---|---|
| $O_3$ | 40 |

**Table 8: Microwindow list for $O_3$**

| Center Wavenumber ($cm^{-1}$) | Microwindow Width ($cm^{-1}$) | Lower Altitude (km) | Upper Altitude (km) |
|---|---|---|---|
| 922.00 [1] | 4.00 | 5 | 20 |
| 984.98 | 0.35 | 5 | 40 |
| 986.90 | 0.35 | 20 | 40 |
| 988.13 | 0.70 | 5 | 45 |
| 990.97 | 0.60 | 20 | 40 |
| 1022.74 | 0.70 | 45 | 80 |
| 1023.55 | 0.60 | 45 | 95 |
| 1024.45 | 0.30 | 45 | 95 |
| 1025.00 | 0.30 | 45 | 95 |
| 1026.00 | 1.20 | 40 | 85 |
| 1027.10 | 1.00 | 60 | 95 |
| 1028.00 | 0.55 | 45 | 95 |
| 1029.00 | 0.60 | 55 | 95 |
| 1030.05 | 0.60 | 45 | 90 |
| 1045.91 | 0.30 | 40 | 95 |
| 1046.85 | 1.00 | 70 | 85 |
| 1048.10 | 0.80 | 45 | 90 |
| 1049.11 | 0.30 | 45 | 95 |
| 1054.24 | 0.33 | 55 | 95 |
| 1056.04 | 0.52 | 45 | 95 |
| 1057.63 | 0.30 | 55 | 95 |
| 1058.28 | 0.60 | 45 | 95 |
| 1084.22 | 0.34 | 30 | 55 |
| 1104.00 | 0.80 | 5 | 45 |
| 1108.03 | 0.40 | 5 | 45 |
| 1114.84 | 0.18 | 5 | 40 |
| 1115.58 | 0.20 | 5 | 45 |
| 1117.35 | 0.26 | 7 | 45 |
| 1119.20 | 0.38 | 35 | 55 |
| 1119.84 | 0.22 | 5 | 45 |
| 1121.85 | 0.35 | 8 | 45 |
| 1122.44 | 0.45 | 40 | 55 |
| 1122.95 | 0.22 | 5 | 45 |
| 1123.93 | 0.45 | 35 | 55 |
| 1126.00 | 0.40 | 30 | 55 |
| 1127.05 | 0.30 | 30 | 50 |
| 1128.49 | 0.28 | 25 | 45 |

[1] Included to improve results for interferer CFC-12 ($CCl_2F_2$)

**Table 9: Interfering molecule(s) for $O_3$**

| Molecule | Upper Altitude Limit (km) |
|---|---|
| $O_3$ (isotope 2) | 45 |
| $O_3$ (isotope 3) | 45 |
| $CCl_2F_2$ | 20 |

**Table 10: Microwindow list for $N_2O$**

| Center Wavenumber ($cm^{-1}$) | Microwindow Width ($cm^{-1}$) | Lower Altitude (km) | Upper Altitude (km) |
|---|---|---|---|
| 1121.85 | 0.35 | 5 | 35 |
| 1123.93 | 0.45 | 35 | 42 |
| 1134.43 | 0.45 | 5 | 15 |
| 1139.80 | 0.60 | 5 | 20 |
| 1168.82 | 0.60 | 5 | 22 |
| 1169.71 | 0.50 | 5 | 22 |
| 1203.82 | 0.65 | 5 | 25 |
| 1204.72 | 0.45 | 5 | 15 |
| 1208.25 | 0.28 | 5 | 22 |
| 1262.85 | 0.35 | 30 | 40 |
| 1264.82 | 0.30 | 30 | 43 |
| 1274.55 | 0.30 | 32 | 41 |
| 1278.10 | 0.35 | 32 | 41 |
| 1278.94 | 0.30 | 32 | 41 |
| 1861.22 | 0.30 | 10 | 20 |
| 1862.02 | 0.30 | 10 | 22 |
| 1864.68 | 0.40 | 10 | 22 |
| 1865.52 | 0.30 | 12 | 22 |
| 1874.44 | 0.35 | 8 | 20 |
| 1886.78 | 0.35 | 9 | 20 |
| 1906.48 | 0.30 | 30 | 50 |
| 1950.68 | 0.30 | 5 | 30 |
| 2188.17 | 0.35 | 31 | 43 |
| 2190.42 | 0.35 | 33 | 45 |
| 2197.65 | 0.70 | 33 | 50 |
| 2201.75 | 0.35 | 35 | 55 |
| 2203.73 | 0.35 | 35 | 58 |
| 2205.75 | 0.50 | 37 | 56 |
| 2207.56 | 0.35 | 35 | 60 |
| 2208.60 | 0.30 | 37 | 60 |
| 2210.46 | 0.45 | 37 | 60 |
| 2211.34 | 0.30 | 37 | 60 |
| 2214.11 | 0.30 | 35 | 60 |
| 2215.10 | 0.30 | 45 | 60 |
| 2216.00 | 0.30 | 45 | 60 |
| 2217.65 | 0.40 | 40 | 60 |
| 2227.82 | 0.30 | 35 | 50 |
| 2237.60 | 0.30 | 55 | 60 |
| 2442.25 | 0.35 | 22 | 32 |
| 2454.36 | 0.30 | 22 | 32 |
| 2455.24 | 0.35 | 22 | 32 |
| 2456.05 | 0.35 | 22 | 32 |
| 2456.94 | 0.35 | 22 | 31 |
| 2460.32 | 0.35 | 18 | 28 |
| 2461.16 | 0.35 | 12 | 25 |
| 2463.63 | 0.30 | 17 | 28 |

**Table 10: Microwindow list for $N_2O$ (continued)**

| Center Wavenumber ($cm^{-1}$) | Microwindow Width ($cm^{-1}$) | Lower Altitude (km) | Upper Altitude (km) |
|---|---|---|---|
| 2466.19 | 0.35 | 20 | 31 |
| 2466.93 | 0.30 | 20 | 31 |
| 2467.79 | 0.35 | 22 | 32 |
| 2519.02 | 0.35 | 6 | 27 |
| 2521.22 | 0.40 | 5 | 27 |
| 2523.50 | 0.40 | 5 | 27 |
| 2548.17 | 0.35 | 27 | 37 |
| 2549.12 | 0.35 | 27 | 37 |
| 2553.80 | 0.35 | 27 | 37 |
| 2556.41 | 0.30 | 26 | 36 |
| 2558.21 | 0.35 | 28 | 36 |
| 2569.75 | 0.30 | 26 | 36 |
| 2570.58 | 0.30 | 27 | 37 |
| 2572.16 | 0.30 | 26 | 37 |
| 2574.29 | 0.30 | 27 | 37 |
| 2595.13 | 0.35 | 5 | 20 |
| 2596.10 | 0.26 | 5 | 22 |
| 2667.85 | 0.35 | 5 | 25 |

**Table 11: Interfering molecule(s) for $N_2O$**

| Molecule | Upper Altitude Limit (km) |
|---|---|
| $CO_2$ | 51 |
| $O_3$ | 42 |
| $CH_4$ | 27 |

**Table 12: Microwindow list for CO**

| Center Wavenumber ($cm^{-1}$) | Microwindow Width ($cm^{-1}$) | Lower Altitude (km) | Upper Altitude (km) |
|---|---|---|---|
| 1119.20 [1] | 0.38 | 35 | 47 |
| 1121.85 [1] | 0.35 | 5 | 35 |
| 2046.29 | 0.24 | 8 | 25 |
| 2086.37 | 0.40 | 70 | 105 |
| 2092.71 | 0.40 | 47 | 55 |
| 2094.76 | 0.40 | 70 | 105 |
| 2099.08 | 0.40 | 47 | 105 |
| 2115.63 | 0.35 | 65 | 105 |
| 2127.67 | 0.40 | 70 | 105 |
| 2135.54 | 0.40 | 25 | 105 |
| 2139.40 | 0.40 | 15 | 105 |
| 2147.18 | 0.35 | 15 | 105 |
| 2150.93 | 0.30 | 25 | 105 |
| 2154.55 | 0.26 | 27 | 105 |

**Table 12: Microwindow list for CO (continued)**

| Center Wavenumber ($cm^{-1}$) | Microwindow Width ($cm^{-1}$) | Lower Altitude (km) | Upper Altitude (km) |
|---|---|---|---|
| 2158.35 | 0.50 | 28 | 105 |
| 2162.02 | 0.35 | 35 | 105 |
| 2165.64 | 0.30 | 28 | 105 |
| 2169.23 | 0.35 | 30 | 105 |
| 2172.76 | 0.40 | 55 | 105 |
| 2176.35 | 0.30 | 35 | 105 |
| 2179.77 | 0.40 | 60 | 105 |
| 2183.20 | 0.40 | 40 | 105 |
| 2189.93 | 0.35 | 40 | 105 |
| 2193.30 | 0.35 | 55 | 105 |
| 2200.00 | 0.35 | 55 | 105 |
| 2203.19 | 0.35 | 35 | 105 |
| 2206.43 | 0.28 | 45 | 100 |
| 2667.85 [2] | 0.40 | 5 | 25 |
| 4209.39 | 0.30 | 5 | 15 |
| 4222.88 | 0.40 | 5 | 15 |
| 4227.35 | 0.60 | 5 | 15 |
| 4231.63 | 0.45 | 5 | 15 |
| 4236.05 | 0.45 | 5 | 15 |
| 4248.35 | 0.35 | 5 | 15 |
| 4274.77 | 0.30 | 5 | 15 |
| 4285.12 | 0.50 | 5 | 15 |
| 4288.27 | 0.35 | 7 | 15 |

[1] Included to improve results for interferer $O_3$
[2] Included to improve results for interferer $CH_4$

**Table 13: Interfering molecule(s) for CO**

| Molecule | Upper Altitude Limit (km) |
|---|---|
| $O_3$ | 55 |
| $CH_4$ | 30 |

**Table 14: Microwindow list for $CH_4$**

| Center Wavenumber ($cm^{-1}$) | Microwindow Width ($cm^{-1}$) | Lower Altitude (km) | Upper Altitude (km) |
|---|---|---|---|
| 1245.14 | 0.30 | 39 | 50 |
| 1267.78 | 0.30 | 45 | 60 |
| 1270.73 | 0.30 | 40 | 60 |
| 1283.43 | 0.30 | 50 | 70 |
| 1287.80 | 0.30 | 55 | 70 |
| 1299.89 | 0.30 | 40 | 55 |
| 1302.07 | 0.30 | 45 | 70 |
| 1302.74 | 0.30 | 55 | 70 |

**Table 14: Microwindow list for $CH_4$ (continued)**

| Center Wavenumber ($cm^{-1}$) | Microwindow Width ($cm^{-1}$) | Lower Altitude (km) | Upper Altitude (km) |
|---|---|---|---|
| 1303.63 | 0.35 | 45 | 70 |
| 1304.25 | 0.30 | 40 | 60 |
| 1311.50 | 0.30 | 50 | 60 |
| 1322.08 | 0.30 | 38 | 70 |
| 1327.23 | 0.60 | 35 | 70 |
| 1332.08 | 0.30 | 55 | 70 |
| 1332.48 | 0.30 | 40 | 70 |
| 1332.75 | 0.30 | 55 | 70 |
| 1337.55 | 0.30 | 40 | 60 |
| 1341.68 | 0.35 | 35 | 70 |
| 1342.65 | 0.30 | 55 | 70 |
| 1346.65 | 0.40 | 32 | 57 |
| 1348.00 | 0.35 | 32 | 57 |
| 1350.95 | 0.30 | 30 | 55 |
| 1351.74 | 0.30 | 35 | 55 |
| 1353.10 | 0.40 | 33 | 60 |
| 1356.00 | 0.35 | 35 | 55 |
| 1407.60 | 0.30 | 15 | 30 |
| 1427.60 | 0.35 | 9 | 20 |
| 1439.43 | 0.35 | 10 | 25 |
| 1463.00 | 0.35 | 12 | 25 |
| 2610.20 | 0.35 | 10 | 27 |
| 2613.98 | 0.35 | 20 | 30 |
| 2614.73 | 0.30 | 20 | 33 |
| 2618.27 | 0.35 | 25 | 37 |
| 2622.58 | 0.30 | 20 | 33 |
| 2636.30 | 0.30 | 5 | 20 |
| 2644.72 | 0.35 | 12 | 28 |
| 2650.70 | 0.35 | 5 | 20 |
| 2658.08 | 0.35 | 12 | 28 |
| 2658.60 | 0.35 | 5 | 25 |
| 2664.50 | 0.35 | 17 | 30 |
| 2667.19 | 0.30 | 20 | 30 |
| 2667.47 | 0.35 | 10 | 27 |
| 2667.85 | 0.40 | 5 | 25 |
| 2669.65 | 0.30 | 5 | 20 |
| 2671.30 | 0.30 | 15 | 30 |
| 2671.66 | 0.45 | 5 | 25 |
| 2674.15 | 0.35 | 20 | 32 |
| 2675.62 | 0.30 | 12 | 27 |
| 2691.25 | 0.30 | 25 | 35 |
| 2805.97 | 0.30 | 23 | 33 |
| 2809.02 | 0.30 | 27 | 37 |
| 2820.82 | 0.30 | 25 | 40 |
| 2822.68 | 0.30 | 28 | 43 |
| 2825.05 | 0.30 | 28 | 40 |

**Table 14: Microwindow list for $CH_4$ (continued)**

| Center Wavenumber ($cm^{-1}$) | Microwindow Width ($cm^{-1}$) | Lower Altitude (km) | Upper Altitude (km) |
|---|---|---|---|
| 2828.17 | 0.40 | 30 | 45 |
| 2835.61 | 0.35 | 18 | 31 |
| 2839.48 | 0.50 | 8 | 22 |
| 2841.22 | 0.35 | 15 | 30 |
| 2847.72 | 0.35 | 27 | 43 |
| 2849.25 | 0.30 | 25 | 36 |
| 2857.50 | 0.35 | 10 | 25 |
| 2867.10 | 0.30 | 30 | 40 |
| 2869.53 | 0.30 | 5 | 20 |
| 2888.48 | 0.28 | 25 | 39 |

**Table 15: Microwindow list for NO**

| Center Wavenumber ($cm^{-1}$) | Microwindow Width ($cm^{-1}$) | Lower Altitude (km) | Upper Altitude (km) |
|---|---|---|---|
| 1104.93 [1] | 0.30 | 15 | 35 |
| 1842.95 | 0.30 | 60 | 110 |
| 1846.62 | 0.30 | 15 | 110 |
| 1850.20 | 0.30 | 45 | 110 |
| 1853.70 | 0.30 | 35 | 110 |
| 1857.17 | 0.45 | 15 | 110 |
| 1860.75 | 0.30 | 60 | 110 |
| 1864.30 | 0.30 | 55 | 105 |
| 1887.53 | 0.40 | 15 | 110 |
| 1890.80 | 0.40 | 40 | 110 |
| 1894.00 | 0.45 | 15 | 110 |
| 1897.00 | 0.35 | 40 | 110 |
| 1900.00 | 0.30 | 15 | 110 |
| 1903.17 | 0.35 | 15 | 110 |
| 1906.15 | 0.30 | 60 | 110 |
| 1909.13 | 0.30 | 60 | 110 |
| 1911.98 | 0.35 | 15 | 110 |
| 1914.96 | 0.30 | 15 | 110 |
| 1917.82 | 0.30 | 85 | 110 |
| 1920.70 | 0.30 | 30 | 55 |
| 1923.46 | 0.24 | 25 | 45 |

[1] Included to improve results for interferer $O_3$

**Table 16: Interfering molecule(s) for NO**

| Molecule | Upper Altitude Limit (km) |
|---|---|
| $O_3$ | 35 |

**Table 17: Microwindow list for $NO_2$**

| Center Wavenumber ($cm^{-1}$) | Microwindow Width ($cm^{-1}$) | Lower Altitude (km) | Upper Altitude (km) |
|---|---|---|---|
| 1581.20 | 0.60 | 15 | 35 |
| 1584.15 | 0.50 | 14 | 35 |
| 1584.70 | 0.40 | 14 | 37 |
| 1585.40 | 0.90 | 14 | 38 |
| 1586.45 | 0.30 | 14 | 38 |
| 1588.70 | 0.30 | 13 | 37 |
| 1590.61 | 0.28 | 14 | 39 |
| 1592.57 | 0.30 | 14 | 40 |
| 1595.33 | 0.40 | 15 | 41 |
| 1597.10 | 0.50 | 14 | 58 |
| 1598.12 | 0.35 | 13 | 58 |
| 1599.93 | 0.55 | 30 | 58 |
| 1602.25 | 0.30 | 15 | 58 |
| 1607.99 | 0.58 | 30 | 58 |
| 1611.70 | 0.40 | 15 | 58 |
| 1628.73 | 0.44 | 25 | 58 |
| 1629.75 | 0.70 | 20 | 58 |
| 1630.97 | 0.30 | 15 | 58 |
| 1634.05 | 0.60 | 28 | 58 |
| 1636.88 | 0.40 | 28 | 58 |
| 1641.65 | 0.30 | 18 | 58 |

**Table 18: Microwindow list for $HNO_3$**

| Center Wavenumber ($cm^{-1}$) | Microwindow Width ($cm^{-1}$) | Lower Altitude (km) | Upper Altitude (km) |
|---|---|---|---|
| 868.10 | 2.20 | 5 | 32 |
| 872.90 | 2.20 | 5 | 32 |
| 878.50 | 3.00 | 15 | 35 |
| 1691.64 | 0.30 | 12 | 32 |
| 1698.25 | 0.70 | 25 | 37 |
| 1701.70 | 0.30 | 25 | 37 |
| 1703.05 | 0.40 | 22 | 37 |
| 1705.31 | 0.60 | 20 | 37 |
| 1716.23 | 0.30 | 25 | 37 |
| 1720.15 | 0.35 | 25 | 35 |
| 1720.89 | 0.40 | 25 | 35 |
| 1728.28 | 0.70 | 10 | 32 |

**Table 19: Interfering molecule(s) for $HNO_3$**

| Molecule | Upper Altitude Limit (km) |
|---|---|
| $H_2O$ | 35 |
| $O_3$ | 35 |
| $N_2O$ | 20 |
| $CH_4$ | 20 |

**Table 20: Microwindow list for HF**

| Center Wavenumber ($cm^{-1}$) | Microwindow Width ($cm^{-1}$) | Lower Altitude (km) | Upper Altitude (km) |
|---|---|---|---|
| 1815.78 [2] | 0.30 | 25 | 35 |
| 1987.34 [1] | 0.30 | 10 | 30 |
| 2010.70 [2] | 0.30 | 10 | 25 |
| 2667.47 [4] | 0.35 | 10 | 23 |
| 2814.40 [3] | 0.30 | 10 | 25 |
| 3788.33 | 0.40 | 10 | 44 |
| 3833.71 | 0.40 | 18 | 48 |
| 3877.75 | 0.35 | 10 | 50 |
| 3920.39 | 0.30 | 27 | 50 |
| 4001.03 | 0.30 | 10 | 50 |
| 4038.87 | 0.45 | 10 | 50 |
| 4109.94 | 0.35 | 25 | 46 |
| 4142.97 | 0.40 | 15 | 40 |

[1] Included to improve results for interferer $H_2O$
[2] Included to improve results for interferer $O_3$
[3] Included to improve results for interferer $N_2O$
[4] Included to improve results for interferer $CH_4$

**Table 21: Interfering molecule(s) for HF**

| Molecule | Upper Altitude Limit (km) |
|---|---|
| $H_2O$ | 30 |
| $O_3$ | 35 |
| $N_2O$ | 25 |
| $CH_4$ | 23 |

**Table 22: Microwindow list for HCl**

| Center Wavenumber ($cm^{-1}$) | Microwindow Width ($cm^{-1}$) | Lower Altitude (km) | Upper Altitude (km) |
|---|---|---|---|
| 2701.26 | 0.30 | 8 | 36 |
| 2703.03 | 0.30 | 35 | 47 |
| 2727.77 | 0.40 | 8 | 45 |
| 2751.97 | 0.30 | 47 | 55 |
| 2775.75 | 0.30 | 40 | 55 |
| 2798.95 | 0.35 | 51 | 57 |
| 2819.48 | 0.30 | 20 | 54 |
| 2821.47 | 0.30 | 18 | 57 |
| 2841.63 | 0.40 | 20 | 50 |
| 2843.67 | 0.30 | 15 | 57 |
| 2865.16 | 0.26 | 38 | 57 |
| 2906.30 | 0.30 | 45 | 57 |
| 2923.57 | 0.50 | 20 | 48 |
| 2923.73 | 0.30 | 44 | 50 |
| 2925.90 | 0.30 | 17 | 57 |
| 2942.67 | 0.40 | 15 | 54 |
| 2944.95 | 0.30 | 10 | 57 |
| 2961.00 | 0.40 | 25 | 48 |
| 2963.11 | 0.50 | 8 | 57 |
| 2981.00 | 0.50 | 40 | 57 |
| 2995.88 | 0.30 | 45 | 51 |
| 2998.14 | 0.30 | 52 | 57 |

**Table 23: Interfering molecule(s) for HCl**

| Molecule | Upper Altitude Limit(km) |
|---|---|
| $O_3$ | 40 |
| $CH_4$ | 50 |

**Table 24: Microwindow list for OCS**

| Center Wavenumber ($cm^{-1}$) | Microwindow Width ($cm^{-1}$) | Lower Altitude (km) | Upper Altitude (km) |
|---|---|---|---|
| 2038.90 | 0.20 | 7 | 20 |
| 2043.50 | 0.40 | 10 | 25 |
| 2045.14 | 0.30 | 7 | 25 |
| 2048.05 | 0.35 | 10 | 25 |
| 2052.72 | 0.30 | 10 | 25 |

**Table 25: Interfering molecule(s) for OCS**

| Molecule | Upper Altitude Limit(km) |
|---|---|
| $O_3$ | 25 |
| $CO_2$ | 25 |

**Table 26: Microwindow list for $N_2O_5$**

| Center Wavenumber ($cm^{-1}$) | Microwindow Width ($cm^{-1}$) | Lower Altitude (km) | Upper Altitude (km) |
|---|---|---|---|
| 1225.00 | 30.00 | 15 | 40 |
| 1255.00 | 30.00 | 15 | 40 |

**Table 27: Interfering molecule(s) for $N_2O_5$**

| Molecule | Upper Altitude Limit (km) |
|---|---|
| $CH_4$ | 40 |
| $N_2O$ | 40 |
| $H_2O$ | 40 |
| $CO_2$ | 40 |

**Table 28: Microwindow list for $ClONO_2$**

| Center Wavenumber ($cm^{-1}$) | Microwindow Width ($cm^{-1}$) | Lower Altitude (km) | Upper Altitude (km) |
|---|---|---|---|
| 780.15 | 0.60 | 12 | 20 |
| 1104.93 [1] | 0.30 | 12 | 35 |
| 1202.86 [2] | 0.50 | 12 | 18 |
| 1292.60 | 1.60 | 18 | 35 |
| 1728.28 [3] | 0.50 | 12 | 18 |

[1] Included to improve results for interferer $O_3$
[2] Included to improve results for interferers $N_2O$ and $CH_4$
[3] Included to improve results for interferer $HNO_3$

**Table 29: Interfering molecule(s) for $ClONO_2$**

| Molecule | Upper Altitude Limit (km) |
|---|---|
| $O_3$ | 12 |
| $HNO_3$ | 33 |
| $N_2O$ | 35 |
| $CH_4$ | 35 |

**Table 30: Microwindow list for HCN**

| Center Wavenumber ($cm^{-1}$) | Microwindow Width ($cm^{-1}$) | Lower Altitude (km) | Upper Altitude (km) |
|---|---|---|---|
| 1438.70 | 0.30 | 10 | 28 |
| 1444.76 | 0.30 | 15 | 25 |
| 3261.75 | 0.30 | 7 | 15 |
| 3268.25 | 0.30 | 7 | 22 |
| 3277.86 | 0.30 | 7 | 26 |
| 3281.02 | 0.30 | 8 | 26 |
| 3287.30 | 0.40 | 7 | 28 |
| 3296.48 | 0.26 | 10 | 28 |
| 3299.56 | 0.30 | 8 | 26 |
| 3305.54 | 0.35 | 7 | 22 |
| 3328.77 | 0.30 | 20 | 28 |
| 3334.30 | 0.30 | 13 | 28 |

**Table 31: Microwindow list for $CH_3Cl$**

| Center Wavenumber ($cm^{-1}$) | Microwindow Width ($cm^{-1}$) | Lower Altitude (km) | Upper Altitude (km) |
|---|---|---|---|
| 2966.50 | 0.40 | 9 | 25 |
| 2966.90 | 0.40 | 9 | 25 |
| 2967.30 | 0.70 | 9 | 25 |

**Table 32: Interfering molecule(s) for $CH_3Cl$**

| Molecule | Upper Altitude Limit (km) |
|---|---|
| $O_3$ | 25 |
| $CH_4$ | 25 |

**Table 33: Microwindow list for $CF_4$**

| Center Wavenumber ($cm^{-1}$) | Microwindow Width ($cm^{-1}$) | Lower Altitude (km) | Upper Altitude (km) |
|---|---|---|---|
| 1283.20 | 2.00 | 20 | 45 |

**Table 34: Interfering molecule(s) for $CF_4$**

| Molecule | Upper Altitude Limit (km) |
|---|---|
| $CH_4$ | 45 |
| $N_2O$ | 45 |

**Table 35: Microwindow list for $CCl_2F_2$ (CFC-12)**

| Center Wavenumber ($cm^{-1}$) | Microwindow Width ($cm^{-1}$) | Lower Altitude (km) | Upper Altitude (km) |
|---|---|---|---|
| 922.00 | 4.00 | 6 | 28 |
| 1161.00 | 1.20 | 12 | 25 |

**Table 36: Interfering molecule(s) for $CCl_2F_2$ (CFC-12)**

| Molecule | Upper Altitude Limit (km) |
|---|---|
| $O_3$ | 25 |
| $N_2O$ | 25 |

**Table 37: Microwindow list for $CCl_3F$ (CFC-11)**

| Center Wavenumber ($cm^{-1}$) | Microwindow Width ($cm^{-1}$) | Lower Altitude (km) | Upper Altitude (km) |
|---|---|---|---|
| 842.50 | 25.00 | 5 | 22 |

**Table 38: Interfering molecule(s) for $CCl_3F$ (CFC-11)**

| Molecule | Upper Altitude Limit (km) |
|---|---|
| $CO_2$ | 22 |
| $HNO_3$ | 22 |
| $H_2O$ | 22 |
| $O_3$ | 22 |

**Table 39: Microwindow list for $COF_2$**

| Center Wavenumber ($cm^{-1}$) | Microwindow Width ($cm^{-1}$) | Lower Altitude (km) | Upper Altitude (km) |
|---|---|---|---|
| 1950.27 | 1.36 | 10 | 32 |
| 1952.05 | 1.20 | 10 | 32 |

**Table 40: Interfering molecule(s) for $COF_2$**

| Molecule | Upper Altitude Limit (km) |
|---|---|
| $H_2O$ | 32 |
| $CO_2$ | 32 |
| $O_3$ | 32 |

**Table 41: Microwindow list for $C_2H_6$**

| Center Wavenumber ($cm^{-1}$) | Microwindow Width ($cm^{-1}$) | Lower Altitude (km) | Upper Altitude (km) |
|---|---|---|---|
| 2976.95 | 0.60 | 6 | 14 to 21 |

**Table 42: Interfering molecule(s) for $C_2H_6$**

| Molecule | Upper Altitude Limit (km) |
|---|---|
| $O_3$ | 14 to 21 |

**Table 43: Microwindow list for $C_2H_2$**

| Center Wavenumber ($cm^{-1}$) | Microwindow Width ($cm^{-1}$) | Lower Altitude (km) | Upper Altitude (km) |
|---|---|---|---|
| 3268.50 | 0.30 | 5.0 to 8.0 | 8.5 to 14.5 |
| 3295.78 | 0.30 | 5.0 to 8.0 | 9.5 to 14.5 |
| 3305.10 | 0.50 | 4.0 to 6.5 | 9.5 to 14.5 |

**Table 44: Interfering molecule(s) for $C_2H_2$**

| Molecule | Upper Altitude Limit (km) |
|---|---|
| $H_2O$ | 8.5 to 14.5 |

**Table 45: Microwindow list for $CHF_2Cl$**

| Center Wavenumber ($cm^{-1}$) | Microwindow Width ($cm^{-1}$) | Lower Altitude (km) | Upper Altitude (km) |
|---|---|---|---|
| 809.30 | 1.10 | 5 | 15 |
| 820.85 | 0.70 | 5 | 12 |
| 829.03 | 0.50 | 5 | 25 |

**Table 46: Interfering molecule(s) for $CHF_2Cl$**

| Molecule | Upper Altitude Limit (km) |
|---|---|
| $O_3$ | 25 |
| $CO_2$ | 25 |

**Table 47: Microwindow list for $SF_6$**

| Center Wavenumber ($cm^{-1}$) | Microwindow Width ($cm^{-1}$) | Lower Altitude (km) | Upper Altitude (km) |
|---|---|---|---|
| 947.65 | 0.90 | 7 | 22 |

**Table 48: Interfering molecule(s) for $SF_6$**

| Molecule | Upper Altitude Limit (km) |
|---|---|
| $CO_2$ | 22 |

**Table 49: Microwindow list for ClO**

| Center Wavenumber ($cm^{-1}$) | Microwindow Width ($cm^{-1}$) | Lower Altitude (km) | Upper Altitude (km) |
|---|---|---|---|
| 823.475 | 5.00 | 11 | 30 |
| 828.475 | 5.00 | 11 | 30 |
| 833.475 | 5.00 | 11 | 30 |
| 838.475 | 5.00 | 11 | 30 |
| 843.475 | 5.00 | 11 | 30 |

**Table 50: Interfering molecule(s) for ClO**

| Molecule | Upper Altitude Limit (km) |
|---|---|
| $CHF_2Cl$ | 30 |
| $CCl_3F$ | 30 |

**Table 51: Microwindow list for $HO_2NO_2$**

| Center Wavenumber ($cm^{-1}$) | Microwindow Width ($cm^{-1}$) | Lower Altitude (km) | Upper Altitude (km) |
|---|---|---|---|
| 802.89 | 2.08 | 12 | 25 |

**Table 52: Microwindow list for $H_2O_2$**

| Center Wavenumber ($cm^{-1}$) | Microwindow Width ($cm^{-1}$) | Lower Altitude (km) | Upper Altitude (km) |
|---|---|---|---|
| 1233.10 | 4.60 | 5 | 12 |

**Table 53: Microwindow list for HOCl**

| Center Wavenumber ($cm^{-1}$) | Microwindow Width ($cm^{-1}$) | Lower Altitude (km) | Upper Altitude (km) |
|---|---|---|---|
| 1221.21 | 0.46 | 10 | 30 |
| 1227.50 | 2.25 | 10 | 30 |
| 1232.03 | 2.54 | 10 | 30 |
| 1234.66 | 2.16 | 10 | 30 |

**Table 54: Microwindow list for $N_2$**

| Center Wavenumber ($cm^{-1}$) | Microwindow Width ($cm^{-1}$) | Lower Altitude (km) | Upper Altitude (km) |
|---|---|---|---|
| 2388.35 | 0.24 | 20 | 35 |
| 2395.96 | 0.28 | 15 | 35 |
| 2403.55 | 0.35 | 15 | 40 |
| 2411.13 | 0.35 | 15 | 35 |
| 2418.63 | 0.35 | 20 | 40 |
| 2426.14 | 0.40 | 15 | 30 |
| 2433.64 | 0.24 | 15 | 37 |
| 2440.97 | 0.35 | 15 | 30 |

**Table 55: Interfering molecule(s) for $N_2$**

| Molecule | Upper Altitude Limit (km) |
|---|---|
| $CO_2$ | 30 |
| $N_2O$ | 30 |

Tables in this appendix (Appendix C: Microwindow List) are from the document *ACE-SOC-0020: Microwindow Lists for ACE-FTS Retrievals – Version 2.2 + Updates*